

Polyhydroxyalkanoate synthesis by mixed microbial consortia cultured on fermented dairy manure: Effect of aeration on process rates/yields and the associated microbial ecology

Erik R. Coats^{a,*}, Benjamin S. Watson^{b,1}, Cynthia K. Brinkman^a

^a Department of Civil Engineering, University of Idaho, Moscow, ID 83844-1022, USA

^b Brown and Caldwell, Seattle, WA, USA

ARTICLE INFO

Article history:

Received 5 August 2016

Received in revised form

19 September 2016

Accepted 20 September 2016

Available online 21 September 2016

Keywords:

Polyhydroxyalkanoates

PHA

Volatile fatty acids

VFAs

Aerobic dynamic feeding

ADF

Next generation sequencing

Oxygen mass transfer coefficient

ABSTRACT

Polyhydroxyalkanoates (PHAs) are biodegradable polymers that can substitute for petroleum-based plastics in a variety of applications. One avenue to commercial PHA production involves coupling waste-based synthesis with the use of mixed microbial consortia (MMC). In this regard, production requires maximizing the enrichment of a MMC capable of feast-famine PHA synthesis, with the metabolic response induced through imposition of aerobic-dynamic feeding (ADF) conditions. However, the concept of PHA production in complex matrices remains unrefined; process operational improvements are needed, along with an enhanced understanding of the MMC. Research presented herein investigated the effect of aeration on feast-famine PHA synthesis, with four independent aeration state systems studied; MMC were fed volatile fatty acid (VFA)-rich fermented dairy manure. Regardless of the aeration state, all MMC exhibited a feast-famine response based on observed carbon cycling. Moreover, there was no statistical difference in PHA synthesis rates, with q_{PHA} ranging from 0.10 to 0.19 CmmolPHA gVSS⁻¹ min⁻¹; VFA uptake rates exhibited similar statistical indifferences. PHA production assessments on the enriched MMC resulted in maximum intracellular concentrations ranging from 22.5 to 90.7% (mgPHA mgVSS⁻¹); at maximum concentration, the mean hydroxyvalerate mol content was $73 \pm 0.6\%$. While a typical feast-famine dissolved oxygen (DO) pattern was observed at maximum aeration, less resolution was observed at decreasing aeration rates, suggesting that DO may not be an optimal process monitoring parameter. At lower aeration states, nitrogen cycling patterns, supported by molecular investigations targeting AOBs and NOBs, indicate that NO₂ and NO₃ sustained feast-famine PHA synthesis. Next-generation sequencing analysis of the respective MMC revealed numerous and diverse genera exhibiting the potential to achieve PHA synthesis, suggesting functional redundancy embedded in the diverse MMC. Ultimately, results demonstrate that aeration can be controlled in waste-based ADF systems to sustain PHA production potential, while enriching for a diverse MMC that exhibits potential functional redundancy. Reduced aeration could also enhance cost competitiveness of waste-based PHA production, with potential further benefits associated with nitrogen treatment.

© 2016 Elsevier Ltd. All rights reserved.

1. Introduction

Biologically-based products are of increasing interest due to their potentially lower environmental impact relative to synthetic alternatives, as well as their foundation on renewable resources. In

* Corresponding author.

E-mail address: ecoats@uidaho.edu (E.R. Coats).

¹ At the time of the research was a graduate student in the Department of Civil Engineering, University of Idaho, Moscow, ID, USA.

particular, plastics of biological origin have gathered significant attention in recent years (e.g., (Chen and Patel, 2012)), with a principal focus on the production of polylactic acid (PLA), starch-based polymers, and polyhydroxyalkanoates (PHAs) (Yates and Barlow, 2013). PLA is synthesized through a combination of chemical and biological processes, with corn being the principal substrate to provide the necessary sugar building blocks; while PLA is of biological origin, it exhibits generally poor biodegradability (Rudnik, 2008). Thermoplastic starch (TPS) production is a chemically-based process, often involving use of a plasticizer; TPS exhibits good biodegradability (Rudnik, 2008). In contrast to PLA

and TPS, PHA is exclusively a biological process, and exhibits excellent biodegradability. Moreover, PHA can more universally be substituted for petro-plastics (Shen et al., 2010), with applications including films, utensils, and packaging (Madison and Huisman, 1999).

Functionally, PHA is an intracellular, amorphous granule synthesized by bacteria as a carbon and energy storage reserve (Serafim et al., 2008). However, in a desiccated state PHA, is a biodegradable thermoplastic. Poly-3-hydroxybutyrate (PHB) was the first form of PHA discovered (Lemoigne, 1926), with many additional structures since identified (Madison and Huisman, 1999) including poly-3-hydroxyvalerate (PHV) and the copolymer PHBV. Carbon substrate dictates structure and polymeric properties (Madison and Huisman, 1999). For example, PHB is synthesized with even numbered carbon substrate (e.g., acetate, glucose) and is a stiff, brittle plastic (Padermshoke et al., 2004), while PHBV is synthesized with even and odd numbered carbon substrate (e.g., acetate and propionate), exhibits reduced crystallinity and improved ductility (Luzier, 1992; Padermshoke et al., 2004), and is less prone to thermal degradation during processing (Luzier, 1992).

Despite the intrinsic potential of this useful biopolymer, PHA production cost is impeding extensive market penetration and adoption. The cost of industrially-produced PHA is largely driven by the need to maintain axenic cultures and provide refined carbon substrate (Fernández-Dacosta et al., 2015). Use of waste substrate can reduce the substrate cost considerably (Gurieff and Lant, 2007). Moreover, coupling waste-based PHA synthesis with the use of mixed microbial consortia (MMC; (Dias et al., 2006; Serafim et al., 2008)) presents a potentially optimal commercial model within which success can be realized, particularly considering that many organic-rich waste streams are candidate substrates for the technology. In this regard, the most commonly employed strategy for PHA production using MMC and waste substrate is a three-stage system that comprises feedstock fermentation, enrichment of PHA-producing bacteria, and PHA production (Serafim et al., 2008). The fermentation stage converts organic material in waste feedstocks to volatile fatty acids (VFAs; optimal precursors for PHA synthesis), while the enrichment stage sustains an MMC enriched for PHA-producing bacteria. The production stage uses a fraction of the enriched culture in a fed-batch reactor to generate commercial quantities of PHA. To complete the production process, the PHA-rich biomass is harvested and subjected to polymer extraction and processing. Given that fermentation of most waste substrates generates even and odd carbon VFAs, MMC PHA synthesis commonly yields PHBV.

Realizing commercial PHA quantities using MMC cultured on waste substrate is predicated on maximizing the enrichment of a microbial consortium capable of feast-famine PHA synthesis. Feast-famine PHA synthesis is a metabolic response to aerobic dynamic feeding (ADF) conditions applied to an MMC fed an organic carbon and nutrient-rich substrate. ADF-induced PHA synthesis on VFA-rich substrate is a well-established phenomenon (Dias et al., 2006; Majone et al., 1996); indeed, recent research has identified proteins associated with the metabolic response (Hanson et al., 2016). For a sequencing batch reactor (SBR), ADF conditions are imposed by first providing an MMC with substrate rich in VFAs in a short duration “feast” time period, thereby creating a large substrate gradient in bulk solution. Operating under aerobic conditions, the microbes rapidly convert the substrate to (predominantly) PHA. Conventionally, the feast phase is defined as ending upon consumption of exogenous substrate; thereafter, conditions are referred to as “famine.” By combining short periods of exogenous substrate availability with long periods of exogenous substrate deficiency, PHA-producing bacteria are enriched over non-PHA producing bacteria (Reis et al., 2003; van Loosdrecht et al.,

1997). Additionally, the reduced anabolic capacity realized late in the famine stage impairs growth and induces the storage of excess substrate as PHA in the subsequent feast phase (Dias et al., 2006; Serafim et al., 2008; van Loosdrecht et al., 1997). In the Production reactor, the inoculum is exposed to a sustained feast response to maximize conversion of VFAs to PHA. The feast-famine response is broadly recognized as the most efficient means to produce PHA using mixed microbial consortia (Serafim et al., 2008), and has been observed in multiple studies.

In considering commercial ADF PHA production, a large operational expense is aeration (Akiyama et al., 2003). However, little is known about aeration requirements and the associated effects of reduced oxygen mass transfer (and, intrinsically, reduced residual dissolved oxygen (DO)) on PHA production by MMC. A specific interest is the impact of low residual DO on PHA “feast.” Most ADF PHA research imposes aeration in excess such that oxygen is not a limiting nutrient during the feast period. To the authors’ knowledge, only one other research group has specifically assessed aeration effects on VFA (acetate) conversion to PHA (Third et al., 2003b, 2004). However, while their research demonstrated that increased PHA yield could be achieved through reducing the aeration rate, investigations focused on PHB synthesis within the context of wastewater treatment, not commercial biopolymer production under imposed ADF conditions. In a somewhat related study, Moralejo-Garate et al. (2013) examined the effect of oxygen limitation on PHB production by MMC cultured on pure glycerol under ADF conditions at near-mesophilic temperatures (30 °C); glycogen synthesis was also examined, based on the potential for bacteria to store glycerol via reverse glycolysis. Results showed that aeration, which was controlled based on applied oxygen mass transfer coefficients (k_{La} ; values of 7.4, 11.4, and 15.6 h⁻¹), adversely impacted both PHB and glycogen storage with decreasing k_{La} ; the PHB synthesis rate and associated yield were maximized under maximal DO conditions.

With an aim to contribute toward future ADF PHA commercialization, research was conducted to assess and develop an enhanced understanding of the impacts of aeration on PHA synthesis, yield, and production by MMC cultured on waste substrate (specifically VFA-rich fermented dairy manure); as a further inquiry, the respective MMC were characterized using next-generation sequencing methods. Dairy manure was selected as the target substrate based on the ready availability of sufficient organic carbon for PHA synthesis and also the fact that enhanced waste management practices are needed in the dairy industry to ameliorate environmental challenges while concurrently enhancing industry economics (Coats et al., 2013). Research objectives were to i) establish PHA Enrichment reactors at varying aeration rates (established based on the oxygen mass transfer coefficient, k_{La} , with DO measured as a surrogate response), ii) assess, characterize, and compare Enrichment reactor process performance relative to oxygen mass transfer, iii) establish the potential effects of reduced oxygen mass transfer on ADF PHA production, and iv) evaluate and characterize the MMC ecology across imposed aeration conditions.

2. Materials and methods

2.1. PHA enrichment reactors

Four bench-scale PHA Enrichment reactors were operated for this research (Table 1); reactor identification was based on the applied oxygen mass transfer coefficient, k_{La} (e.g., AE-4 was operated at a k_{La} of 4 h⁻¹). All reactors were operated as SBRs, were continuously stirred with no settling phase, and were operated with an SRT and HRT of 4 days and cycle length of 24 h. Aeration

Table 1
Experimental reactor operating conditions.

| Reactor | Operating volume (L) | k_{La} (hr^{-1}) | Air flow (mL min^{-1}) | Avg. Flow reduction from AE-20 | SRT and HRT (d) |
|---------|----------------------|-------------------------------|-----------------------------------|--------------------------------|-----------------|
| AE-4 | 1.2 | 4 | 15 | 97.5% | 4 |
| AE-8 | 1.2 | 8 | 80 | 87% | 4 |
| AE-12 | 1.2 | 12 | 245 | 59% | 4 |
| AE-20 | 1.2 | 20 | 600 | NA | 4 |

was accomplished with a 2.0- μm gas sparger (Williams Brewing, San Leandro CA, USA); air flow rates (Table 1) were controlled using Aera PI-98 mass flow controllers (MFC's) rated to $0\text{--}1000 \pm 1$ standard cubic cm per min (sccm) (Hitachi Metals America, San Jose, California, USA). Mixing was achieved with Thermo Scientific Cimarec magnetic stir plates (Thermo Fisher Scientific Inc., Waltham, MA, USA) and 3.8 cm TeflonTM coated magnetic stir bars. The reactors were scrubbed daily; the aeration stones were soaked in 1N HCl for a minimum of 5 min each day, rinsed with deionized water, cleaned with Kimwipe[®], and then re-submerged in the reactor. After reactor cleaning, 300 mL of mixed liquor was removed and either disposed of or used in a PHA Production reactor. Each reactor was then re-filled with 300 mL of substrate comprised of 40% dairy manure fermenter liquor and 60% tap water by volume; the resultant organic loading rate was $0.44 \pm 0.11 \text{ gCOD}_{\text{VFA}} \text{ L}^{-1} \text{ d}^{-1}$ ($12.5 \pm 3.2 \text{ Cmmol L}^{-1} \text{ d}^{-1}$; $n = 19$). The applied OLR was approximately an order of magnitude lower than Dionisi et al. (2006) but comparable to that of Dionisi et al. (2001, 2004). For this study, batches of substrate were mixed every three days and stored at 4 °C until use. Tap water was added prior to feeding and cleaning to compensate for evaporation. Enrichment reactors were operated at ambient room temperature (22–25 °C).

2.2. Quantification of aeration rate

The aeration rate in MMC PHA studies is commonly reported as volume of air provided per reactor volume or as a surrogate based on DO concentration, while some just report the equipment used. Such approaches are acceptable when PHA reactors are excessively aerated to ensure oxygen is not limiting the targeted biochemical reaction; this condition is typical for most PHA investigations. However, properly quantifying aeration characteristics is important if the research is to be ultimately transferred to full-scale, particularly considering that aeration costs must be minimized.

Aeration in this study was controlled based on the universal oxygen mass transfer coefficient, k_{La} . Oxygen uptake rate (OUR) and k_{La} were determined in accordance with the dynamic degassing method (García-Ochoa and Gomez, 2009). The k_{La} was measured during the famine phase of the Enrichment reactor cycle to prevent VFA catabolism from influencing the OUR. As part of the k_{La} quantification, air flow to the reactor was first stopped and the DO was allowed to decrease to approximately 2 mg L^{-1} . Once the DO reached 2 mg L^{-1} , air flow was returned to the reactor and the DO concentrations recorded. The k_{La} coefficient with the best fit was quantified using the residual squared sum of errors (with an R^2 greater than 0.999). k_{La} was corrected for temperature based on the van't Hoff-Arrhenius relationship using $Q = 1.024$ (Tchobanoglous et al., 2014). Operational k_{La} values for all Enrichment reactors were confirmed every two weeks, at a minimum; in addition, prior to process assessment, k_{La} values were confirmed both seven and one day prior to testing.

2.3. Effects of wastewater characteristics on aeration

The relative oxygen transfer efficiency of each reactor was quantified based on the parameter α , normalizing the k_{La} for

wastewater to the k_{La} for tap water (Tchobanoglous et al., 2014). To quantify α , the wastewater k_{La} was first corrected to 20 °C. The tap water k_{La} was measured in the same reactor and with the same aeration apparatus; sodium sulfite and cobalt chloride were used to remove oxygen from solution. α values were 1.1 (AE-4), 0.88 (AE-8), 1.01 (AE-12), and 0.98 (AE-20), respectively.

2.4. PHA production reactors

All PHA Production reactors had an initial operational volume of 300 mL (i.e., the daily waste from the respective Enrichment reactors), and investigations were conducted using undiluted dairy manure fermenter liquor. The same aeration stones and mixing plates were used as in the Enrichment reactors. During operation of the PHA Production reactors, DO was monitored continuously. The aeration rate was not controlled; instead, air flow rate was set so that DO concentration exceeded 1.0 mg L^{-1} , such that oxygen was not a limiting nutrient in the biochemical reactions.

The PHA production potential of inocula obtained from the Enrichment reactors was evaluated in four discrete stages (identified as 1-A, -B, followed by 2-A, -B). For stage 1-A and 1-B operations, the PHA Production reactors were pulsed with substrate following a spike in residual DO or at a set time interval (45 min for 1-A, 30 min for 1-B) if DO did not otherwise indicate a need for more substrate. The time interval selection was based on the previous day Enrichment reactor VFA uptake rate and VFA concentration of the Production reactor substrate. Each pulse volume was held volumetrically constant at 10% of reactor volume at time of pulse. Operational stages 2-A and 2-B employed a 30 min feeding interval, with 30 mL of substrate supplied per pulse. The mass of VFAs added for each interval in stages 2-A and -B was designed to ensure that the empirical maximum bulk solution VFA concentration of 60 Cmmol L^{-1} (Serafim et al., 2004) was not exceeded.

2.5. Source of manure; dairy manure fermenter operations

Raw dairy manure was collected from the University of Idaho dairy every 7–14 days, sampled for total solids (TS) and volatile solids (VS) content at the time of collection, and stored at 4 °C until use. Manure was collected to minimize contamination with refractory lignocellulosic bedding material.

The fermented dairy manure liquor for the PHA investigations was obtained from a bench-scale dairy manure fermenter; manure characteristics and fermenter operational conditions are detailed in Stowe et al. (2015). Briefly, a 22.7 L fermenter was operated at a volume of 20 L, a 4 d SRT and HRT, and a target OLR of $8.75 \text{ gVS L}^{-1} \text{ d}^{-1}$, with feeding and wasting conducted once per day. The target OLR was maintained based on the VS samples collected from the raw manure. Fermentation took place at room temperature (22–25 °C). Fermenter mixing was accomplished using a 9.5 cm diameter helical impeller driven by an Oriental Motor (USM315-401W 15 W AC; San Jose, CA, USA) connected to a 3GN35SA reduction gearbox. Fermenter liquor was obtained via centrifugation of the fermenter effluent at 8000 rpm for 5 min at room temperature to separate liquid and solid fractions. Fermenter liquor characteristics for the period of operations associated with this

study were as follows ($n = 26$): 2410 ± 470 mgCOD_{HAc} L⁻¹, 1230 ± 1720 mgCOD_{HPr} L⁻¹, 982 ± 238 mgCOD_{HBU} L⁻¹, 456 ± 53 mgCOD_{HVa} L⁻¹, and 41 ± 27 mgCOD_{HCA} L⁻¹. In a previous study (Hanson et al., 2016) the VFA fraction (COD basis) of dairy manure fermenter liquor was estimated at 70%; based on Enrichment reactor effluent data, the non-biodegradable fraction was approximately 10% (Passero et al., 2014). Limited analysis on nutrients showed ammonia-N ranging from 448 to 1143 mgN L⁻¹ and orthophosphate ranging from 25 to 131 mgP L⁻¹; thus, the fermenter liquor substrate was not macronutrient deficient.

2.6. Analytical techniques

PHA content was analyzed as methyl ester derivative through GC/MS, applying a modification of the method originally proposed (Braunegg et al., 1978). Samples were treated with 1 mL of commercial sodium hypochlorite to lyse the cells, then centrifuged at 10 000 rpm for 4 min. Supernatant was removed and the remaining solids rinsed with deionized water twice. Biomass was dried at 100–105 °C for a minimum of 24 h. 10–20 mg of dried biomass was weighed into a test tube for digestion along with 2 mL of methanol acidified with H₂SO₄ (3% vol basis) and 1 mL of chloroform with 0.5 mg L⁻¹ benzoic acid (internal standard). The sample was digested for 4 h at 100 °C in a Hach DRB 200 digestion block (Hach Company, Loveland CO, USA). Samples were allowed to cool before adding 2 mL of deionized water, then vortexed for 30 s. The samples stabilized for a minimum of 5 min to allow the organic and aqueous phases to separate. The organic phase was pipetted and filtered through a Pasteur pipette column of anhydrous sodium sulfate into a 2 mL screw top glass vial with Teflon[®]-sealed cap (Thermo Fisher Scientific Inc., Waltham, MA, USA). Samples were injected into a ThermoQuest Trace[™] GC with a Finnigan PolarisQ iontrap using a ThermoQuest AS2000 autosampler (Thermo Fisher Scientific Inc., Waltham, MA, USA). The inlet was operated in split mode, with a temperature of 210 °C. Separation was achieved using a ZB1 (30 m × 0.25 mm ID) capillary column (Phenomenex, Torrance, CA, USA) which was ramped from an initial 40 °C to 200 °C at 5 °C min⁻¹. 3-hydroxybutyrate and 3-hydroxyvalerate monomers were verified by mass spectra at 103 m/z and retention time matching based on commercial standards (Sigma-Aldrich Co., St. Louis, MO, USA). The standard curves for quantification had correlation coefficients of $R^2 > 0.95$ (3-Hydroxyvalerate) and $R^2 > 0.98$ (3-Hydroxybutyrate).

VFAs (acetic, propionic, butyric, isobutyric, valeric, isovaleric, and caproic acids) and methanol were quantified using a Hewlett-Packard 6890 series gas chromatograph (GC) (Agilent Technologies, Inc., Santa Clara, CA, USA) equipped with a flame-ionization detector (FID) and a Hewlett-Packard 7679 series injector. The system was interfaced with the Hewlett-Packard GC ChemStation software version A.06.01. VFA separation was achieved using a capillary column (Heliflex[®] AT[™]-AquaWax-DA, 30 m × 0.25 mm ID, W. R. Grace & Co., Deerfield, IL, USA) which was ramped from an initial 50 °C–200 °C in three steps (2 min at 50 °C, ramp to 95 °C at 30 °C min⁻¹ then to 150 °C at 10 °C min⁻¹ and hold for 3 min; finally, ramp to 200 °C at 25 °C min⁻¹ and hold for 12 min) with helium as the carrier gas (1.2 mL min⁻¹). The split/splitless injector and detector were operated isothermally at 210 and 300 °C, respectively. Prior to analysis, samples were acidified to a pH of 2 using nitric acid. 0.5 µL of each sample was injected in 20:1 split mode. VFA concentrations were determined through retention time matching with known standards (Sigma-Aldrich Co., St. Louis, MO, USA; Thermo Fisher Scientific Inc., Waltham, MA, USA) and linear standard curves ($R^2 > 0.99$).

For soluble constituents, samples were first centrifuged to remove solids/biomass and then filtered through a 0.22 µm syringe

filter (Millipore Corp., Billerica, MA, USA). Soluble NO₃-N was determined in accordance with Hach method 10020. Soluble NH₄-N testing followed Hach method 10031. Soluble NO₂-N was determined using Hach method 8153 and method 8507. A Spectronic[®] 20 Genesys[™] spectrophotometer (Thermo-Fisher Scientific Corp, Waltham, MA, USA) was utilized to measure the absorbance of the reacted sample. Soluble reactive phosphorus was determined in accordance with Hach (Loveland, CO, USA) method 8048 (method equivalent to Standard Methods 4500-PE (Clesceri et al., 1998)). Nutrient concentrations were determined utilizing appropriate standard curves ($R^2 > 0.99$).

Dissolved oxygen (DO) was measured using a Hach IntelliCAL[™] LDO101 probe connected to a Hach HQ40d Multi-Parameter Meter. Data was logged using the USB and AC power adapter. TS and VS were measured following Standard Methods 2540D and 2540E respectively (APHA et al., 2012).

2.7. Quantitative polymerase chain reaction (qPCR)

qPCR was applied to estimate the relative abundance of ammonia oxidizing bacteria (AOB) and nitrite oxidizing bacteria (NOB) in the Enrichment reactors. Bulk genomic DNA from each reactor was extracted using a PowerSoil[®] DNA Extraction Kit (MO BIO Laboratories Inc., Carlsbad, CA USA). Genomic DNA yield and purity was quantified using a Synergy H1 Multi-Mode Reader (BioTek, Winooski, VT). qPCR was conducted on a StepOne Plus[™] Real-Time PCR system (Applied Biosystems, Foster City, CA) using iTaq[™] SYBR[®] Green Supermix w/ROX (Bio-Rad Laboratories, Inc., Hercules, CA, USA) and a total reaction volume of 25 µL. Eubacteria were amplified using primer sets developed by Muyzer et al. (1993). Amplification of AOBs was based on a primer set for the gene ammonia monooxygenase (*amoA*) (Rotthauwe et al., 1997). For NOBs, *Nitrobacter* spp. and *Nitrospira* were amplified using 16S rDNA sequences. qPCR settings were in accordance with Winkler et al. (2011). AOB, *Nitrobacter*, and *Nitrospira* abundance relative to eubacteria was estimated using the mean efficiencies for each primer set and the C_q values for the individual samples, assuming average 16S rDNA gene copy numbers of 4.1 for eubacteria, 2.5 for AOB (Leininger et al., 2006), and 1.0 for both *Nitrobacter* and *Nitrospira* (McIlroy et al., 2015). All samples were assessed in triplicate with 5 ng of total genomic DNA per reaction. qPCR melting curves were evaluated to confirm a single melting peak, and agarose gel analysis confirmed a single band for each primer set. Amplification efficiencies were calculated for each primer set using baseline-corrected fluorescence data (StepOne software v2.0), and the LinRegPCR program (Ramakers et al., 2003). The cycle threshold was set at a constant value across all samples based on location within the log-linear region for determination of C_q values (cycle number at which the measured fluorescence exceeds the cycle threshold).

2.8. DNA sequence analysis and taxonomic classification

Illumina sequencing was performed on genomic DNA recovered from the respective PHA Enrichment reactors on three operational days. Bacterial 16S rRNA gene fragments were amplified and sequenced in accordance with Hanson et al. (2016). DNA amplicons were generated using two PCR rounds (round one amplified the targeted region of the 16S rRNA gene and round two attached sequencing adapters and sample barcodes) for eubacteria (Shen et al., 2016); the primers are described in Hanson et al. (2016). The barcoded amplicons were sequenced using an Illumina MiSeq instrument creating paired end 2 × 300 bp libraries (Illumina, Inc., San Diego, CA).

Sequence analysis and taxonomic classification were performed

following Hanson et al. (2016). Briefly, the Illumina MiSeq reads were demultiplexed and assigned to expected barcode and primer sequences using the Python script dbcAmplicons (<https://github.com/msettles/dbcAmplicons>). After the primer sequences were trimmed, the reads were joined into a single amplicon sequence using the application FLASH (Magoč and Salzberg, 2011). The Ribosomal Database Project (RDP) Naïve Bayesian classifier was then used to assign the joined sequences to phylotypes (Wang et al., 2007); assignment was made to the lowest taxonomic rank with a bootstrap score $\geq 50\%$. The relative abundance of individual phylotypes in each sample was determined as the percentage of the corresponding sequence reads among the total sequence reads in the sample.

2.9. Data analysis

Custom software (altvisngs; available at <https://github.com/nguho/altvisngs>) was used to quantify the sample diversity and evenness indices, complete the rarefaction and hierarchical cluster analysis, and generate the taxon hierarchy with relative abundance, heatmap, and summary bar plot images (see Supplementary Data). Single factor ANOVA was used to establish differences in means using Microsoft Excel, with significance declared at $p < 0.05$.

3. Results and discussion

The performance of mixed microbial consortia (MMC) in each unique aeration-state PHA Enrichment reactor was evaluated for both PHA synthesis and production potential. The PHA Enrichment reactors were operated for a period of 271 days, with detailed performance interrogations conducted on operational days 19, 52, 144, 190, and 271. In addition, PHA production evaluations were conducted on operational days 173, 238, 263, and 271. Results from the Enrichment reactor investigations are presented and discussed below first, with Production evaluations presented thereafter.

3.1. Aeration effects on PHA synthesis

As described, the PHA Enrichment reactors were operated identically with the exception of the experimental variable: the aeration rate, which was established based on the applied oxygen mass transfer coefficient, k_La , and measured based on residual DO. Four aeration rates were examined: $k_La = 4, 8, 12$, and 20 h^{-1} . While these applied aeration rates aligned with a comparative study of Third et al. (2003b); $k_La = 6\text{--}51 \text{ h}^{-1}$ and were similar to a PHB-focused study that used a differing substrate (glycerol) (Moralejo-Gárate et al., 2013), applied values were less than the minimum k_La of 120 h^{-1} recommended by Dias et al. (2006) for MMCs producing PHA on waste substrate.

First considering VFA utilization patterns – which, coupled with PHA synthesis patterns, indicate the presence or absence of an induced feast-famine response – results confirm the targeted response was in fact induced regardless of the applied aeration state (Fig. 1). In all Enrichment reactors the time required for complete VFA utilization ranged from approximately 50 min to approximately 120 min, which is consistent with similar ADF PHA studies (Beun et al., 2002; Serafim et al., 2004). More importantly, PHA synthesis patterns were comparable across the four enrichment reactors (Fig. 2a–d). Ultimately, the observed PHA synthesis on VFAs under the applied ADF conditions and across the four aeration states was consistent with feast-famine theory (Dias et al., 2006). All consortia exhibited a maximum PHA concentration approaching $10\text{--}15 \text{ Cmmol L}^{-1}$ and comparable lowest peak concentrations of approximately $3\text{--}5 \text{ Cmmol L}^{-1}$. Average intracellular concentrations (gPHA gTSS^{-1}) were similar across aeration states,

as was the variability over the tested operational days. Comparing results, there was no statistical difference in average PHA yield, although it does appear that VFA conversion to PHA was more efficient under higher aeration states (Table 2).

DO has been suggested as a surrogate parameter that could be monitored in real-time to establish the end of the PHA feast period (Beun et al., 2002; Dias et al., 2005; Serafim et al., 2004); the importance of this real-time feedback relates to downstream PHA production, in that DO could be used as an indicator that famine conditions are impending and thus more VFAs are needed to sustain the feast and maximize PHA synthesis. Examining DO for all Enrichment reactors revealed important results (Fig. 2). A typical ADF response would exhibit a DO “valley” during the feast phase and immediately after receiving new substrate, followed by a rapid increase in residual DO as the MMC enters a famine period (and the microorganisms can more readily manage available electrons for growth). Indeed, the biomass realizing the highest aeration rate (AE-20) exhibited a typical feast-famine DO response (Fig. 2a), with both initial ($t = 0$) and famine residual DO concentrations approaching saturation, while the DO concentration during the feast phase averaged $1.25 \pm 0.99 \text{ mg L}^{-1}$. At the other aeration extreme (reactor AE-4; Fig. 2d), atypical DO conditions were observed. Specifically, while a DO “valley” was observed, the residual DO remained generally less than 2 mg L^{-1} well beyond the end of the feast period (which occurred consistently less than 150 min into the operational cycle; Fig. 1d) and thus did not strongly signal onset of famine conditions. While the DO ultimately increased to approximately 6.5 mg L^{-1} at the end of the SBR cycle (data not shown), the typical feast-famine DO pattern was not observed. Similarly, the middle two aeration rates exhibited atypical feast-famine DO profiles, in that the DO more slowly increased during the famine period (but also ultimately realized an end of cycle DO ranging from 5.7 to 7 mg L^{-1}). Results thus suggest that, depending on the imposed aeration state, DO may not be an ideal candidate for real-time process monitoring of the targeted feast-famine response.

Process kinetics (VFA consumption and PHA synthesis rates (Table 3)) were interrogated to illuminate potential impacts of aeration rate on the PHA Enrichment reactor biomass. First considering VFA consumption rates, the average rate of VFA utilization (r_{VFA}) ranged from 0.20 (AE-12) to 0.31 (AE-20) $\text{CmmolVFA L}^{-1} \text{ min}^{-1}$, while the specific rate of VFA utilization (q_{VFA}) ranged from 0.14 (AE-12) to 0.26 (AE-20) $\text{CmmolVFA gVSS}^{-1} \text{ min}^{-1}$. Regarding PHA synthesis, observed r_{PHA} values ranged from 0.13 (AE-4, 8) to 0.23 (AE-20) $\text{CmmolPHA L}^{-1} \text{ min}^{-1}$; q_{PHA} ranged from 0.10 (AE-8) to 0.19 (AE-20) $\text{CmmolPHA gVSS}^{-1} \text{ min}^{-1}$. For all sets of kinetic data, there was no statistical difference between the respective averages. Moreover, specific rates were higher than observed by Third et al. (2003b) for comparable aeration rates. Third et al. (2003b) observed a residual DO during VFA feast of 0 mg L^{-1} ; conversely, microaerophilic conditions were generally maintained in this study (Fig. 2). Certainly the lack of DO during “feast” in the study by Third et al. (2003b) could have adversely impacted the rates in question. Comparing results with studies wherein aeration induced near-saturation conditions (as summarized in Beun et al. (2002) and observed by Serafim et al. (2004)), this study's q_{VFA} and q_{PHA} values were within the lower observed range (although these other referenced studies used pure acetate as substrate, not a complex waste substrate), while yield values were comparable. While k_La was varied across the Enrichment reactors, more importantly during the carbon flux feast period the residual DO across the four Enrichment reactors did not vary substantially (Fig. 2), which likely explains why the respective rates exhibited no statistical differences. Although Third et al. (2003b) observed that VFA utilization rates and PHA synthesis rates decrease with reduced

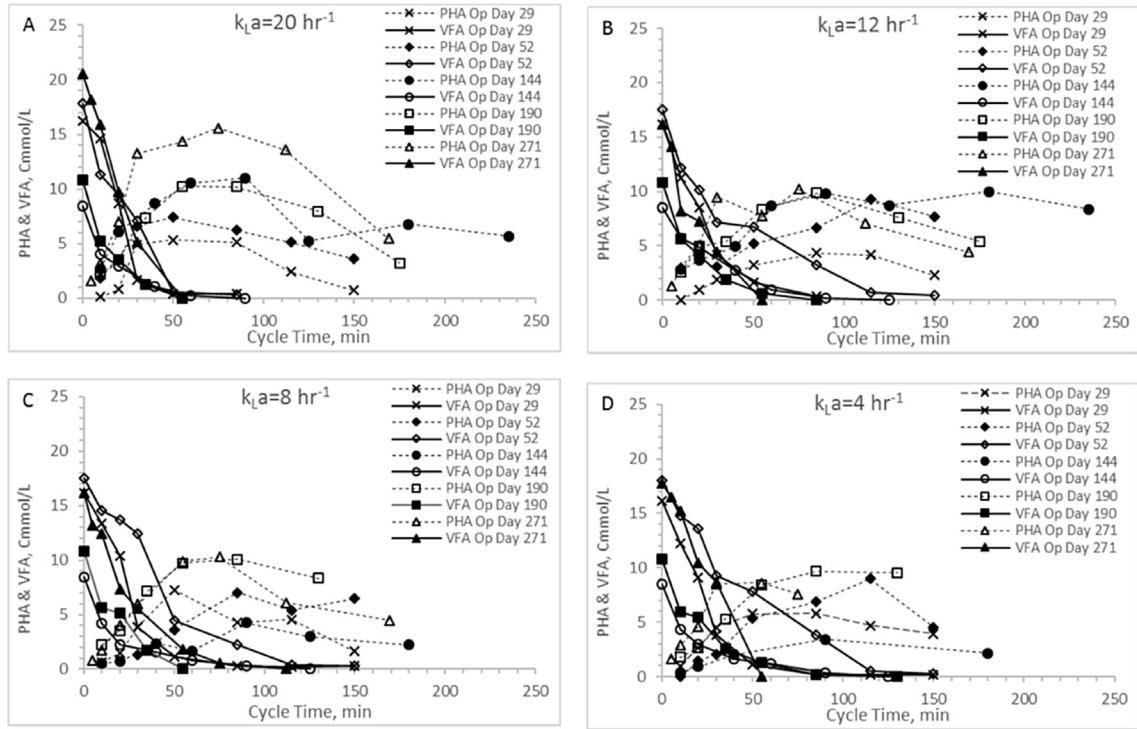


Fig. 1. VFA and PHA profiles for the Enrichment reactors operated at oxygen mass transfer coefficients ($k_L a$) of 20 h^{-1} (a), 12 h^{-1} (b), 8 h^{-1} (c), and 4 h^{-1} (d). Note that PHA reserves at the end of the SBR cycle were depleted.

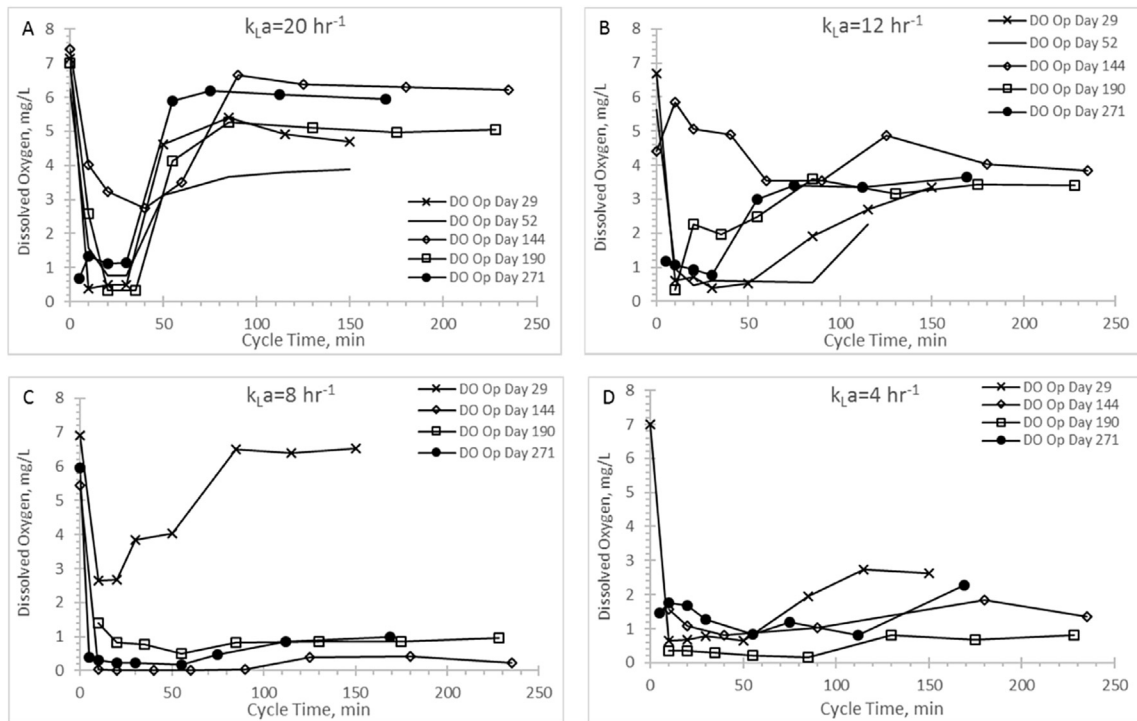


Fig. 2. Residual dissolved oxygen profiles for the Enrichment reactors during the feast phase and into the famine phase for reactors operating at oxygen mass transfer coefficients ($k_L a$) of 20 h^{-1} (a), 12 h^{-1} (b), 8 h^{-1} (c), and 4 h^{-1} (d).

$k_L a$, in comparison with this study, fully anaerobic conditions were realized at the lowest $k_L a$'s.

Although there was no statistically significant difference between observed carbon flux and utilization rates across the

imposed aeration states, the average highest rates (for both VFA uptake and PHA synthesis) occurred in the reactor with the greatest aeration rate (reactor AE-20). Conversely, the MMC in reactor AE-4 (lowest $k_L a$) exhibited the lowest uptake rates. Overall, the VFA and

Table 2
PHA synthesis performance summary in the Enrichment reactors. Results for PHA Yield, PHA_{max}, and %PHA_{max} represent values at maximum observed intracellular PHA concentration. Average %HV represents the average HV content in the PHA throughout the feast phase and subsequent PHA utilization during the famine phase.

| k _{La} (h ⁻¹) | Operational day | PHA yield (CmmolPHA (CmmolVFA) ⁻¹) | | PHA _{max} (Cmmol L ⁻¹) | | %PHA _{max} (gPHA gTSS ⁻¹) | | Avg. HV% (mol basis) |
|------------------------------------|-----------------|--|-------------|---|-------------|--|--------------|----------------------|
| | | | avg. ± SD | | avg. ± SD | | avg. ± SD | |
| 4 | 29 | 0.36 | 0.53 ± 0.21 | 5.81 | 7.31 ± 2.61 | 7.32 | 10.55 ± 4.54 | 35.9 ± 16.8 (n = 32) |
| | 52 | 0.51 | | 8.98 | | 17.10 | | |
| | 144 | 0.41 | | 3.44 | | 5.50 | | |
| | 190 | 0.90 | | 9.68 | | 10.39 | | |
| | 271 | 0.49 | | 8.61 | | 12.45 | | |
| 8 | 29 | 0.46 | 0.59 ± 0.21 | 7.29 | 7.79 ± 2.48 | 10.25 | 10.74 ± 3.60 | 30.8 ± 15.8 (n = 36) |
| | 52 | 0.41 | | 7.02 | | 12.85 | | |
| | 144 | 0.50 | | 4.28 | | 5.57 | | |
| | 190 | 0.93 | | 10.07 | | 9.86 | | |
| | 271 | 0.63 | | 10.28 | | 15.17 | | |
| 12 | 29 | 0.27 | 0.70 ± 0.34 | 4.33 | 8.73 ± 2.48 | 4.41 | 10.90 ± 4.05 | 25.7 ± 19.7 (n = 37) |
| | 52 | 0.54 | | 9.25 | | 12.60 | | |
| | 144 | 1.16 | | 10.00 | | 11.24 | | |
| | 190 | 0.92 | | 9.88 | | 10.81 | | |
| | 271 | 0.63 | | 10.18 | | 15.44 | | |
| 20 | 29 | 0.34 | 0.75 ± 0.39 | 5.34 | 9.92 ± 3.90 | 6.85 | 14.12 ± 6.17 | 38.0 ± 15.9 (n = 38) |
| | 52 | 0.42 | | 7.41 | | 12.50 | | |
| | 144 | 1.30 | | 11.01 | | 18.27 | | |
| | 190 | 0.95 | | 10.26 | | 10.65 | | |
| | 271 | 0.76 | | 15.60 | | 22.33 | | |

Table 3
Rates of VFA uptake and PHA synthesis in the Enrichment reactors (n = 5 per reactor) through the feast phase.

| k _{La} | q _{VFA} (Cmmol gVSS ⁻¹ min ⁻¹) | r _{VFA} (Cmmol L ⁻¹ min ⁻¹) | q _{PHA} (Cmmol gVSS ⁻¹ min ⁻¹) | r _{PHA} (Cmmol L ⁻¹ min ⁻¹) |
|-----------------|--|---|--|---|
| 4 | 0.18 ± 0.07 | 0.22 ± 0.09 | 0.11 ± 0.07 | 0.13 ± 0.09 |
| 8 | 0.20 ± 0.09 | 0.26 ± 0.05 | 0.10 ± 0.04 | 0.13 ± 0.06 |
| 12 | 0.14 ± 0.07 | 0.20 ± 0.08 | 0.11 ± 0.09 | 0.14 ± 0.10 |
| 20 | 0.26 ± 0.13 | 0.31 ± 0.14 | 0.19 ± 0.10 | 0.23 ± 0.12 |

PHA specific rates were variable over time, potentially due to changes in bacterial populations (see also Section 3.5). However, specific PHA synthesis rates by MMCs have been commonly observed to be quite variable, and rates reported herein are well within observed ranges (Beun et al., 2002; Reis et al., 2003).

One final metric to assess the relative magnitude (and to a certain degree efficiency) of a feast-famine response, as well as the successful enrichment of PHA-producing bacteria, is the feast-to-famine (F:F) ratio (van Loosdrecht et al., 1997). The F:F ratio is the total length of the feast phase compared to the total length of the operational cycle; a F:F value of 0.2 has been suggested as a potential maximum to sustain a microbial consortium that will accomplish excess PHA storage over growth (Dionisi et al., 2007). All Enrichment reactors realized a F:F ratio less than 0.2, with AE-4, -8, -12, and -20 operating at average F:F ratios of 0.071, 0.068, 0.051, and 0.037, respectively. The highest aeration rate Enrichment reactor realized the lowest F:F ratio, which aligned with the highest observed average VFA utilization rate; considering that AE-20 was operated under the more optimal (relative) redox state, such results would be expected.

In summary, reduced aeration rate exhibited limited impact on VFA utilization or PHA synthesis (kinetically or stoichiometrically) by MMC on the dairy manure-derived VFA-rich substrate in the Enrichment reactors. These findings suggest the opportunity to realize cost savings (and environmental benefit) from reduced aeration for process scale-up. However, before such conclusions can be firmly established, PHA production potential using inocula from the Enrichment reactors must be considered.

3.2. Impact of enrichment reactor aeration rate on PHA production

In considering commercial PHA production, one of the more important process outcomes is peak intracellular PHA content, measured on a dry weight basis and typically expressed as a percentage. PHA purification requires a variety of solvents, depending on the process selected; thus, higher intracellular PHA concentrations will reduce the cost of the PHA per kg produced through reduced chemical usage (Dias et al., 2006; Van Wegen et al., 1998). Examining intracellular PHA concentrations (Table 4), observed values (mgPHA mgTSS⁻¹, % basis) for AE-4, -8, -12, and -20 ranged from 27.8–40.5, 18.3–54.7, 23.3–70.9, 28.3–62.6 (averages of 35.5, 37.4, 45.9, and 41.7, respectively); results are also shown on a VSS basis. While intracellular concentrations were variable within and across the PHA Production reactors, statistically (ANOVA) the Enrichment reactor aeration rate exhibited no impact (p = 0.77). Of note, the highest obtained value of 90.7% (VSS basis) exceeds reported values of 75% (Albuquerque et al., 2010), 77% (Jiang et al., 2012), and 78.5% (Serafim et al., 2004). These other cited experiments were conducted under growth limitation, not in the presence of excess nutrients; moreover, the latter was performed with synthetic feed. Conversely, the research presented herein was conducted on real waste and without any growth limitation (ammonia, phosphorus, oxygen, and substrate all in excess). Valentino et al. (2015) is the closest comparison to this work; they reported VSS weight percent ranging from 50 to 70%. Results from this research are comparable, even outperforming, although with a larger range of realized %PHA content.

In addition to intracellular PHA concentration, the fractional HV content in the polymer is an important metric; increased HV

Table 4

Performance data for PHA production assessments using inocula from the four different aeration-state Enrichment reactors. Y represents the total VFAs consumed up to the maximum observed intracellular PHA concentration. %PHA_{max} represents the maximum observed intracellular concentration during the production assessment. Avg. HV% represents the mol-basis HV content over the full PHA production assessment.

| Reactor | Production test (Op. Day) | Initial MLSS (mg L ⁻¹) | Y (CmmolPHA CmmolVFA ⁻¹) | %PHA _{max} (mgPHA mgTSS ⁻¹) | %PHA _{max} (mgPHA mgVSS ⁻¹) | Avg. HV% (mol basis) |
|---------|---------------------------|------------------------------------|--------------------------------------|--|--|----------------------|
| AE-4 | 1-A (173) | 2590 | 0.78 | 40.5 | 49.4 | 27 ± 5.2 (n = 16) |
| | 1-B (238) | 2520 | 0.72 | 27.8 | 34.3 | 41 ± 11 (n = 18) |
| | 2-A (263) | 1750 | 0.46 | 38.5 | 48.2 | 65 ± 2.9 (n = 6) |
| | 2-B (271) | 1890 | 0.71 | 35.2 | 42.4 | 49 ± 5.4 (n = 6) |
| AE-8 | 1-A (173) | 2740 | 0.97 | 47.0 | 59.6 | 25 ± 5.4 (n = 16) |
| | 1-B (238) | 2490 | 0.77 | 18.3 | 22.5 | 43 ± 10.0 (n = 16) |
| | 2-A (263) | 1960 | 0.91 | 54.7 | 67.9 | 69 ± 0.86 (n = 5) |
| | 2-B (271) | 1780 | 0.68 | 29.7 | 35.3 | 44 ± 3.8 (n = 6) |
| AE-12 | 1-A (173) | 2540 | 0.94 | 43.1 | 52.7 | 31 ± 5.1 (n = 17) |
| | 1-B (238) | 2410 | 0.87 | 23.3 | 29.1 | 42 ± 7.8 (n = 16) |
| | 2-A (263) | 1790 | 1.12 | 70.9 | 90.7 | 73 ± 0.6 (n = 6) |
| | 2-B (271) | 1160 | 0.97 | 46.1 | 54.1 | 52 ± 2.1 (n = 6) |
| AE-20 | 1-A (173) | 1820 | 0.76 | 33.4 | 40.0 | 28 ± 7.8 (n = 16) |
| | 1-B (238) | 2460 | 0.93 | 28.3 | 35.5 | 42 ± 4.8 (n = 19) |
| | 2-A (263) | 1940 | 0.97 | 62.6 | 78.3 | 73 ± 0.52 (n = 5) |
| | 2-B (271) | 1687 | 0.94 | 42.6 | 49.6 | 54 ± 2.6 (n = 6) |

content reduces polymer crystallinity and improves ductility (Luzier, 1992; Padermshoke et al., 2004) while also rendering the PHA less prone to thermal degradation during processing (Luzier, 1992) and expanding commercial applications (Dias et al., 2006). Mean HV content (mol basis) over the duration of all the production evaluations was 0.46 ± 0.16 (n = 46), 0.46 ± 0.18 (n = 44), 0.49 ± 0.18 (n = 45), and 0.49 ± 0.19 (n = 46) for Production reactors AE-4, -8, -12, and -20, respectively; relative HV content within each production assessment is summarized in Table 4. Interestingly, the average HV content was markedly higher in the Production reactor biomass (Table 4) as compared with the Enrichment reactor biomass (Table 2). A closer review of the data indicates that the HV content steadily increased over the duration of a production assessment, and in many cases the HV content during the initial stages of the production campaign were more consistent with that of the associated Enrichment reactor. While a clear explanation on the phenomenon of increasing HV content is not known, considering the complex VFA matrix and the associated metabolisms for conversion of VFAs to PHA (Braunegg et al., 1998), it is plausible that over the production period the MMC more readily oxidized acetate (via acetyl CoA and the TCA cycle), leaving the less readily metabolized VFAs (C3–C5) utilized for PHV synthesis.

As a final analysis regarding the potential impact of Enrichment reactor aeration on PHA production, the mass of carbon required to achieve maximum intracellular PHA concentration was evaluated. This metric was determined at the time point when maximum intracellular PHA concentration was observed, and considers the total VFAs consumed to achieve the peak PHA value. The premise of this interrogation was that the lower aeration state in the Enrichment reactor could render the inocula less metabolically conditioned for hyper-PHA synthesis, and thus potentially more VFA-carbon would be consumed to achieve maximal intracellular PHA concentration. Indeed, a review of the data (Table 4) suggests that PHA production using inocula from AE-4 (lowest aeration state) did in fact require more carbon than the higher aeration states (0.46 – 0.78 CmmolPHA CmmolVFA⁻¹ for AE-4 vs. 0.76 – 0.97 CmmolPHA CmmolVFA⁻¹ for AE-20). Moreover, statistically (ANOVA) the four discrete Production reactor average yields were not equal ($p = 0.048$; although the averages for AE-8, -12, and -20 were statistically equal ($p = 0.24$)). While yield values approaching or exceeding one may seem implausible, such results are not uncommon when using complex wastewater substrates, as summarized by Reis et al. (2003). Moreover, given the complexity of manure (Stowe et al., 2015) and associated upstream process (fermentation), other forms of soluble carbon (e.g., carbohydrates;

long chain fatty acids) were likely present in the fermenter liquor (but not measured) which could have been converted to PHA.

3.3. Assessing PHA production operational strategy

Two different operational methods were evaluated to maximize PHA production using MMC inocula from the Enrichment reactors. The approach to PHA production is to supply excess carbon substrate to a MMC capable of feast-famine PHA synthesis such that a “feast” response is sustained, thereby achieving maximal intracellular PHA accumulation and associated biomass PHA production. Sustaining a “feast” response requires avoiding both substrate inhibition and limitation.

Comparing PHA production strategies, as shown (representative results in Figs. 3 and 4) the method wherein VFAs were pulsed to the biomass every 30 min (Fig. 4) resulted in sustained VFA availability to the MMC and ultimately the highest intracellular PHA concentrations (Table 4; Stages 1 vs. Stages 2 results). The relative HV content was not affected by operational strategy or inocula source, as HV content was similar across all reactors for each production assessment (Table 4). The primary difference between the two operational strategies can be considered as being proactive vs. reactive, related to avoiding a substrate limitation. Applying a DO-based strategy (pulse VFAs when the residual DO increases rapidly) can be considered a reactive strategy, in that substrate is added when the bulk solution concentration is effectively exhausted. As such, depending on the process monitoring and control rigor, for a short duration the microbes can shift reliance to PHA for growth and maintenance. Indeed, such a response can be observed in the data presented in Fig. 3. To avoid PHA consumption while minimizing process control requirements, new substrate can simply be provided to the biomass on a more regular interval in order to sustain a feast response. For this study, 30 min feed intervals facilitated an environment wherein no substrate limitation was realized (Fig. 4). Moreover, the applied operational strategy (feed interval coupled with mass of VFAs added) sustained bulk solution VFA concentrations within the empirical limit to avoid PHA synthesis inhibition (maximum of 60 Cmmol L⁻¹ according to Serafim et al. (2004)). Consequently, improved PHA accumulation was sustained.

3.4. Aeration rate, feast-famine PHA synthesis, and nitrogen cycling

To better understand and potentially explain why reduced aeration rate did not impact PHA synthesis and production,

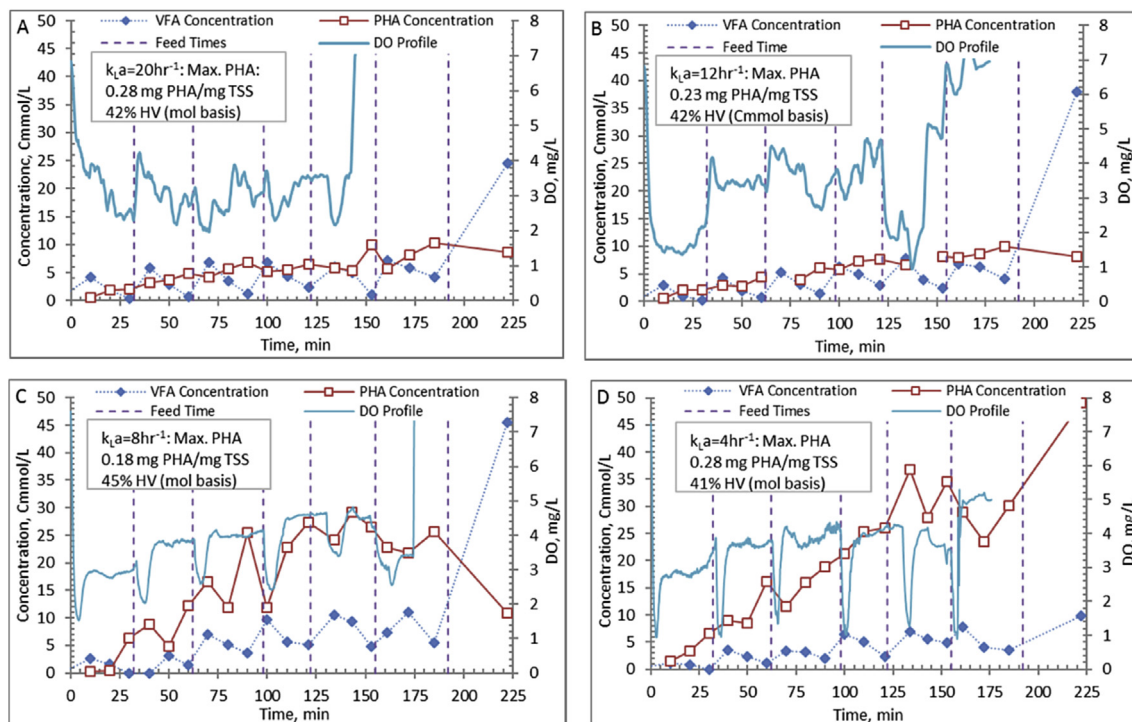


Fig. 3. Example PHA production data (stage 1-B) for biomass from the Enrichment reactors operated at oxygen mass transfer coefficients (k_La) of 20 h^{-1} (a), 12 h^{-1} (b), 8 h^{-1} (c), and 4 h^{-1} (d). Operations were conducted to supply new substrate (VFA-rich fermenter liquor) to the biomass based on a sudden increase in dissolved oxygen.

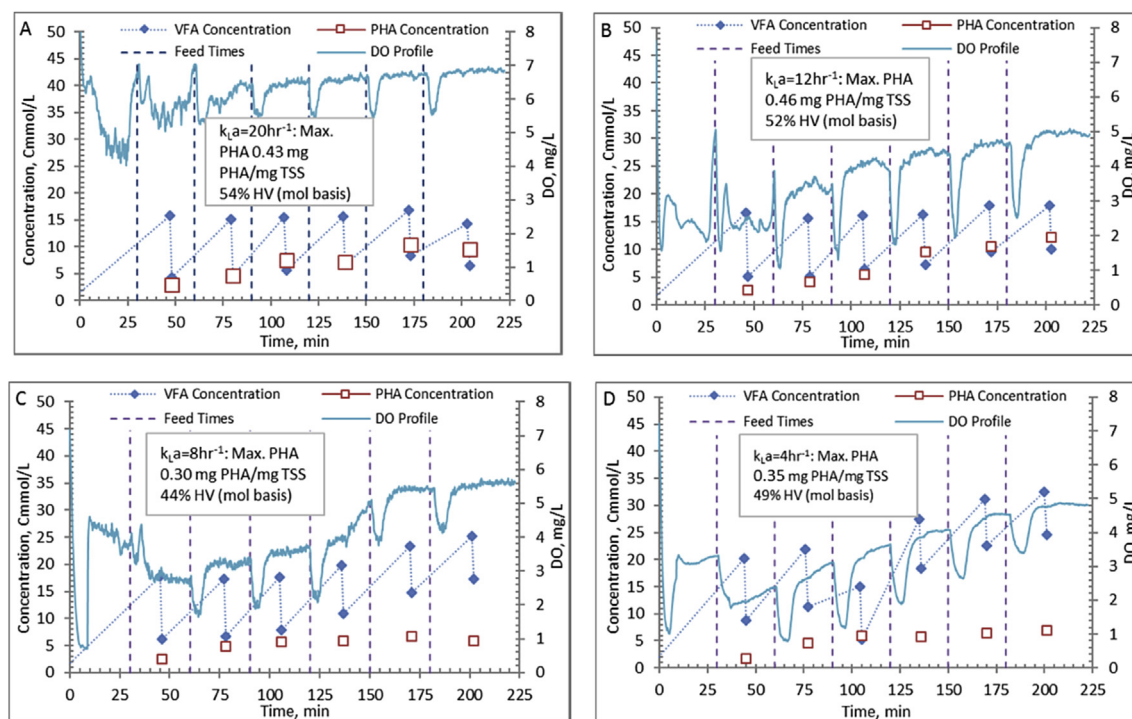


Fig. 4. Example PHA Production data (stage 2-B) for biomass from the Enrichment reactors operated at oxygen mass transfer coefficients (k_La) of 20 h^{-1} (a), 12 h^{-1} (b), 8 h^{-1} (c), and 4 h^{-1} (d). Operations were conducted to supply new substrate (VFA-rich fermenter liquor) to the biomass every 30 min.

nitrogen cycling patterns in the Enrichment reactors were examined. Theoretically, NO_2 and NO_3 (produced through nitrification) could sustain the catabolic and anabolic metabolisms necessary for VFA feast and PHA synthesis; use of NO_2/NO_3 in the presence of

oxygen has been referred to as simultaneous nitrification-denitrification (SND). Note that Enrichment reactor operations did not attempt to actively control or inhibit nitrification, and the fermented dairy manure liquor contained ammonia. [Third et al.](#)

(2003a) observed SND within a feast-famine response, but operational conditions were such that NO_3^- was not available until the famine phase and thus PHB served as the carbon and electron source; thus, Third et al. (2003a) did not observe SND during the feast phase. However, their results suggested that SND could be realized by a PHA producing MMC at DO concentrations less than 1.0 mg L^{-1} ; research presented herein met this DO limit (Fig. 2).

First considering Enrichment reactor AE-20 (highest aeration rate), indeed a significant amount of ammonia oxidation occurred; representative results are presented in Fig. 5a, showing that effluent ammonia (previous cycle) was less than 3 mgN L^{-1} and that nitrification occurred throughout the operational cycle. Regarding NO_2^- and NO_3^- , results (Fig. 5a) suggest that SND during the feast period was not realized at the imposed residual DO concentrations. However, nitrification was partially inhibited (i.e., partial nitrification ($\text{NH}_4 \rightarrow \text{NO}_2^-$); Fig. 5a), in that NO_2^- concentrations increased more significantly than NO_3^- for the first 6–7 h of the operational cycle. Nevertheless, late-cycle nitrification occurred in AE-20, as illustrated by the near-zero preceding-cycle NO_2^- concentrations and correspondingly high NO_3^- concentrations (Fig. 5a). Examining the other aeration extreme (AE-4; Fig. 5b), while again significant ammonia oxidation occurred over the operational cycle, in contrast to AE-20, some NO_2^- and NO_3^- reduction during the feast phase was observed. Specifically, for the Enrichment reactor characterization on operational day 144 (Fig. 5b), both NO_2^- and NO_3^- were reduced to nearly zero after approximately 6 h, with a nominal increase in NO_2^- initially during the low-DO feast period. Similar NO_3^- patterns were observed for the Enrichment reactor characterization on operational day 190, indicating that NO_3^- was used as a terminal electron acceptor to support heterotrophic respiratory metabolic activities; conversely, autotrophic NO_2^- production was realized over the same time period. In contrast to observations for the highest aerated reactor (AE-20), these results indicate that residual NO_3^- from the preceding operational cycle was used by the MMC to sustain a VFA feast (and PHA synthesis), while the aeration state concurrently supported partial nitrification. Results align with recent work on the same substrate (Hanson et al., 2016), as well as PHA production on sugar factory wastewater (Anterrieu et al., 2014).

qPCR was applied to quantify the relative NOB and AOB populations and better understand the bulk solution observations. Regarding the NOB population, the relative fractional abundance of *Nitrobacter* spp. (which exhibit a low affinity for NO_2^- and oxygen) for Enrichment reactors AE-4, -8, -12- and -20 was $1.8 \pm 1.0\%$, $2.6 \pm 2.2\%$, $3.5 \pm 3.5\%$, and $5.9 \pm 4.8\%$, respectively. Relative fractions align with the imposed aeration state, as *Nitrobacter* spp. predominate at elevated residual DO concentrations (i.e., highest for AE-20, lowest for AE-4). In contrast, negligible *Nitrospira* were

detected in any of the Enrichment reactors; *Nitrospira* typically predominate at lower DO concentrations than observed herein. Regarding AOBs, relative concentrations for Enrichment reactors AE-4, -8, -12- and -20 were $0.28 \pm 0.40\%$, $0.95 \pm 1.3\%$, $0.81 \pm 1.7\%$, and $0.43 \pm 0.81\%$, respectively. AOBs exhibit a lower specific growth rate than NOBs and thus would be present in lower concentrations (relative to NOBs). Collectively, these molecular insights affirm the observed bulk solution nitrogen observations ($\text{NH}_4 \rightarrow \text{NO}_2^- \rightarrow \text{NO}_3^-$) and also demonstrate the potential to enrich for flanking microbial populations that can generate alternative electron acceptors to maintain feast-famine PHA production.

As a final observation regarding the observed nitrogen cycling, a secondary benefit arises beyond supporting feast-famine PHA synthesis at a reduced aeration rate. U.S. dairies are increasingly facing nitrogen-based environmental challenges. Thus, concurrent nitrogen treatment would be a significant benefit in addition to commodity PHA production.

3.5. Microbial ecology of the PHA enrichment reactors

To characterize the microbial composition of the MMC in the Enrichment reactors, on three operational days (29, 52, and 271) amplicons of the V1-V3 region of the 16S rRNA gene for Eubacteria were sequenced and assigned to phylotypes. The total number of joined sequences obtained are summarized in Table S1. The number of reads ranged from 29 583–120 133, and sequencing coverage depth was considered sufficient for all samples based on rarefaction analysis (Fig. S1), although there was one lesser quality data set (MMC from reactor AE-12 on operational day 271; Fig. S1c). While MMC in reactors AE-8 and -20 appeared to be somewhat more diverse, all four Enrichment reactors generally exhibited similar complexity (average Shannon index of 3.74–4.18; range of 3.59–4.41; Table S1). The Shannon index was selected for its value as a general complexity measure considering both richness and evenness (Hill et al., 2003).

A comprehensive summary of the eubacterial-based MMC composition from the domain to genus level for each Enrichment reactor is presented in Figs. S8–S23 (see also Tables S8–S37); Fig. 6 presents a summary of the respective MMC's on operational day 271. Focusing on the genera level (Table 5), *Meganema* was the most common and highly abundant genus observed across all samples, ranging from 4.95 to 32.8%; moreover, *Meganema* was the only genus present at >10% in all Enrichment reactors on operational days 29 and 52. However, on operational day 271 *Meganema* decreased to 4.95–6.93% of the population, while *Zoogloea* was the only genus >10% (and only in reactor AE-12). Though *Meganema* has been observed in other ADF enrichment SBRs wherein PHA was synthesized in excess (Hanson et al., 2016; Majone et al., 2006),

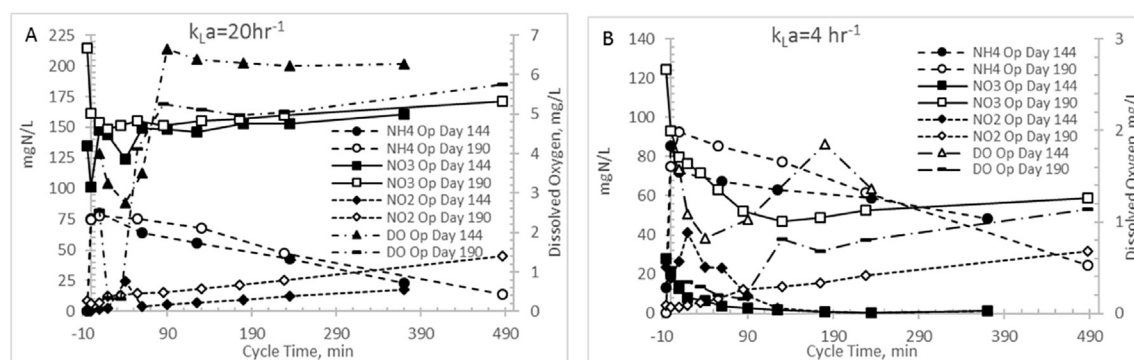


Fig. 5. Nitrogen cycling in Enrichment reactors operated at oxygen mass transfer coefficients ($k_L a$) of 20 h^{-1} (a) and 4 h^{-1} (b). Note that the abscissa scale begins at -10 min to reflect nitrogen concentrations before the cycle operations commenced.

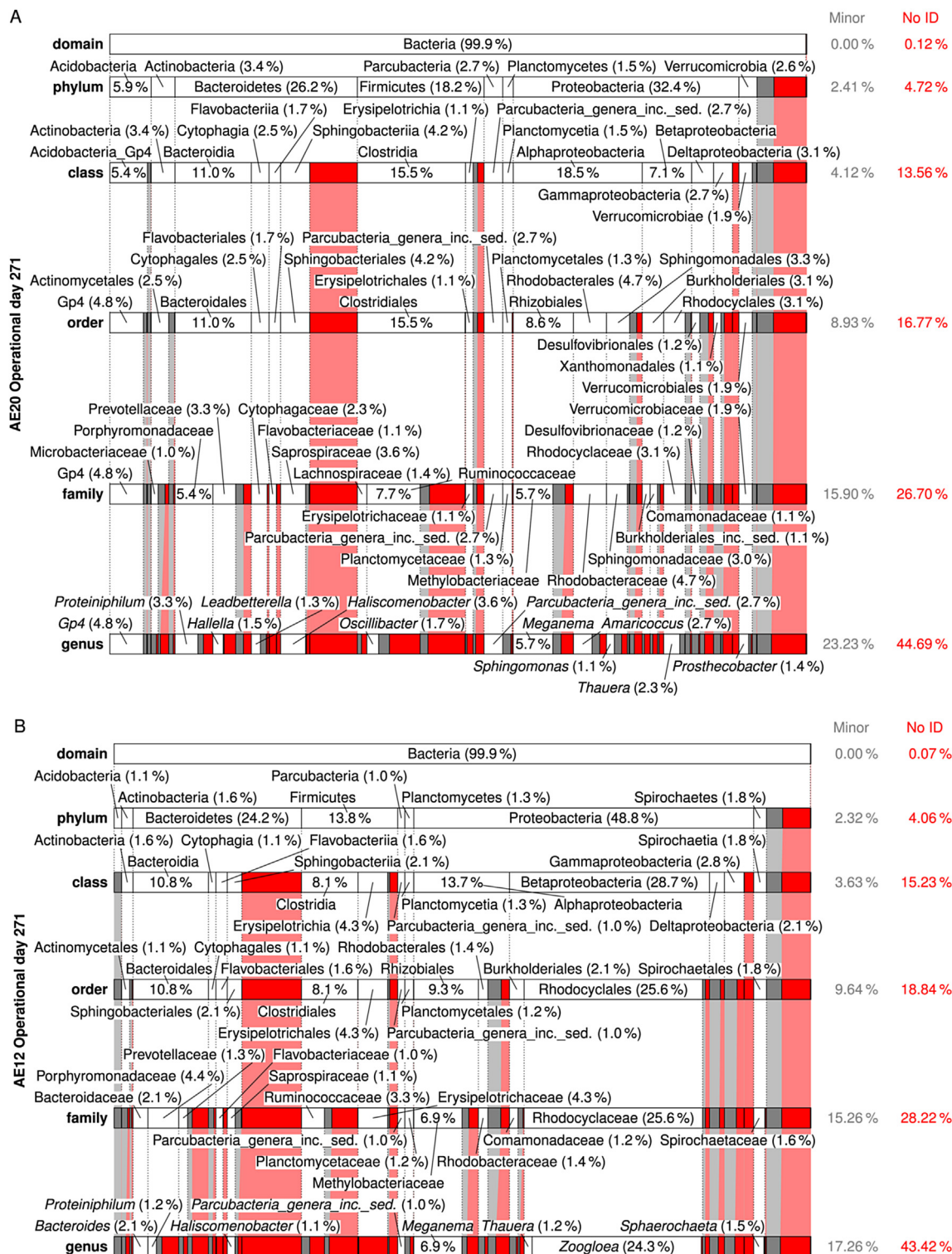


Fig. 6. Relative abundance and taxonomic classification of the 16S rRNA gene sequencing results using the RDP for Enrichment reactors on operational day 271 and operated at oxygen mass transfer coefficients ($k_L a$) of 20 h^{-1} (a), 12 h^{-1} (b), 8 h^{-1} (c), and 4 h^{-1} (d). The classified phylotypes are depicted in terms of the taxonomic hierarchy. Phylotypes which were not identified by the RDP or those whose identification at a specific taxonomic level was not statistically significant were aggregated, denoted "No ID", and depicted in red. Identified phylotypes with less than 1% of the total relative abundance were aggregated, denoted "Minor", and depicted in gray. Phylotypes with at least 1% relative abundance are labeled. (For interpretation of the references to colour in this figure legend, the reader is referred to the web version of this article.)

including with fermented dairy manure as a substrate (Hanson et al., 2016), the high abundance of *Meganema* was in contrast to other ADF studies that reported dominant genera including *Thauera* (Albuquerque et al., 2013; Carvalho et al., 2014; Lemos et al., 2008),

Azoarcus (Bengtsson et al., 2010a, 2010b; Waller et al., 2012), or *Plasticumulans* (Jiang et al., 2011, 2012; Marang et al., 2013). Additionally, most of the genera identified in this study present at >1% (e.g., *Leadbetterella*, *Halscomenobacter*, *Aquabacterium*,

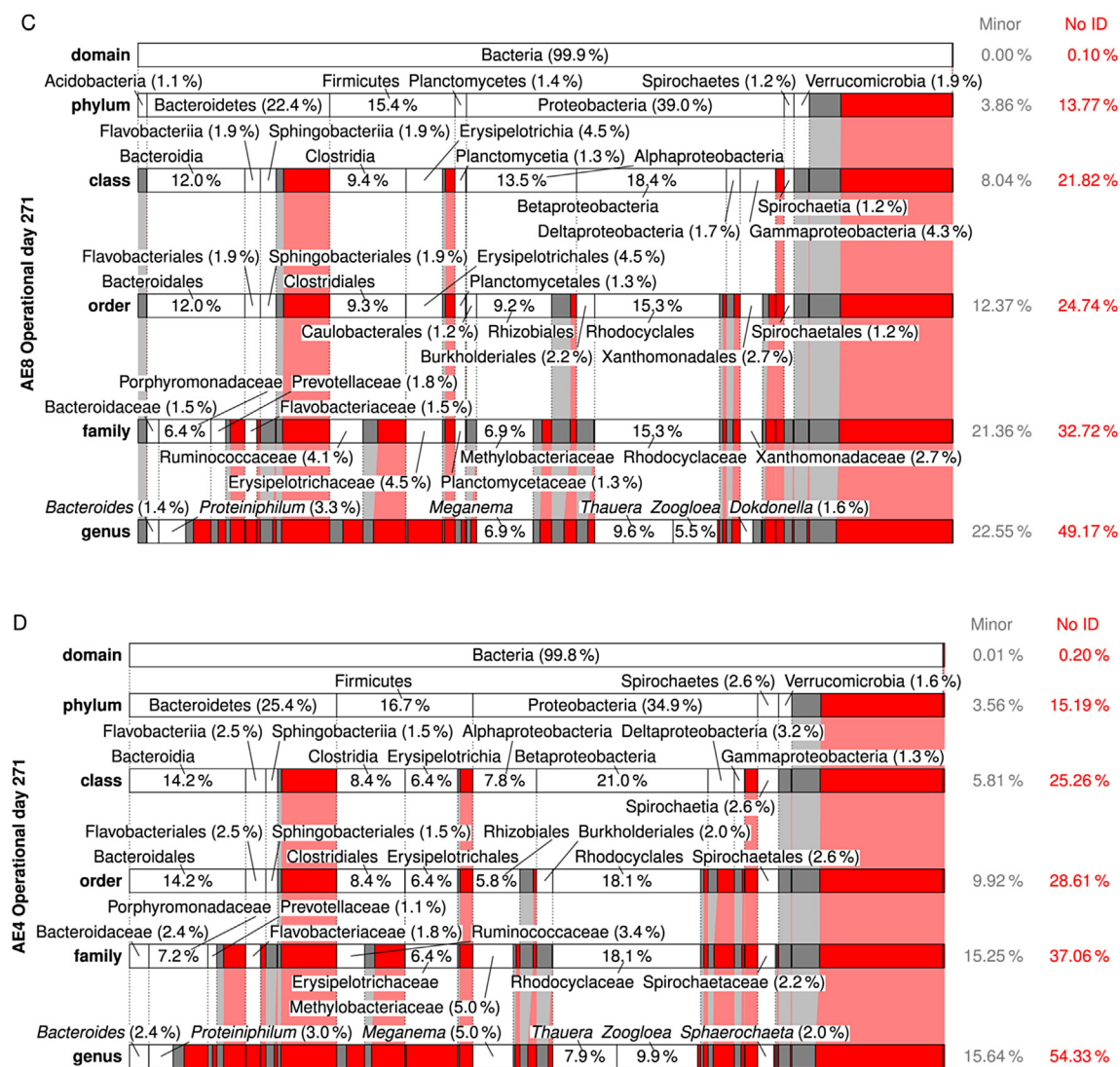


Fig. 6. (continued).

Luteimonas, *Hydrogenophaga*, *Thermomonas*, *Mycobacterium*, *Filomicrobium*, *Dokdonella*, *Hylemonella*, *Pseudofulvimonas*, *Mesorhizobium*, *Hyphomicrobium*, *Parvibaculum*, *Brevundimonas*, *Novosphingobium*, *Sphingomonas*, *Altererythrobacter*, *Xanthobacter*, *Gp6*, and *Gp4*) have not been reported in other ADF investigations; *Amaricoccus* and *Paracoccus* have only been nominally present in ADF systems (Lemos et al., 2008; Queirós et al., 2014). Compared with studies using synthetic medium (Albuquerque et al., 2013; Dionisi et al., 2006; Lemos et al., 2008; Villano et al., 2010), real wastewater-based ADF operations appear to enrich for a much more diverse population of potential PHA producing microorganisms. Indeed, the number of taxa identified in this study was higher compared to these previous studies; moreover, the microbial diversity (based on the Shannon index) was markedly higher than reported for an ADF enrichment SBR cultivated on fermented molasses (Shannon index ≤ 1.0) (Carvalho et al., 2014). High-throughput DNA sequencing (a more sophisticated method as compared to FISH or DGGE DNA band sequencing) may explain the more diverse MMC observed in this study, but other possible explanations for the dissimilarity in microbial composition include differing inoculum sources, feedstock composition, and applied operating conditions.

Independent of the differences in microbial composition across this study and also relative to others, the feast-famine response at a bulk solution-level was observed in the Enrichment reactors, indicating that the microbial composition may not be the strongest determinant in eliciting a feast-famine response. Rather, the functional capabilities of the taxa present may be more pertinent. To explore the functional potential associated with the microbial composition, the major genera (Table 5) during the sampling events were further scrutinized. For the MiSeq analysis, phylotypes were not assigned at the species level, meaning that the associated functional capabilities could not be established with absolute certainty. Thus, PHA synthesis potential of the major genera was determined by i) comprehensive literature search of available databases, ii) the genetic potential as established within the Uniprot database (<http://www.uniprot.org/>) and the ribosomal database project (RDP), or iii) consideration of a subordinate taxa (and their associated physiology) as a surrogate (e.g., as identified through the MiDAS database (McIlroy et al., 2015)). The potential to be capable of PHA synthesis was established if a peer-reviewed study identified the genera or species as so capable, or if a mapped genome was shown to include PHA related genes (e.g., PHA synthase, PHA depolymerase, PhaR (Maehara et al., 2002), etc.). Genera exhibiting

Table 5
Summary of Major (>10%) and Minor (1–10%) genera observed in the four PHA Enrichment reactors on operational days 29, 52, and 271. Genera underlined and in bold text all contain species that exhibit PHA production potential (fraction of the respective MMC shown in parentheses).

| Op. Day | AE-4 | AE-8 | AE-12 | AE-20 |
|---------------------------------|---|--|---|---|
| 29 Major (>10%) Minor (>1%) | <u>Meganema (27%)</u> <u>Leadbetterella (3.54%)</u> , <u>Luteimonas (1.78%)</u> , <u>Haliscomenobacter (1.77%)</u> , Planctomyces, <u>Thauera (1.56%)</u> , <u>Aquabacterium (1.35%)</u> , <u>Gp4 (1.32%)</u> , <u>Altererythrobacter (1.2%)</u> , Schlesneria | <u>Meganema (16.1%)</u> Schlesneria, Blastocatella, <u>Luteimonas (2.12%)</u> , <u>Aquabacterium (1.99%)</u> , <u>Gp4 (1.81%)</u> , Roseimicrobium, <u>Thauera (1.7%)</u> , <u>Leadbetterella (1.61%)</u> , Saccharibacteria_genera_inc_sed, <u>Hydrogenophaga (1.36%)</u> , <u>Paracoccus (1.33%)</u> , Verricomicrobium, <u>Haliscomenobacter (1.09%)</u> | <u>Meganema (19.1%)</u> Saccharibacteria_genera_inc_sed, <u>Thauera (3.98%)</u> , <u>Aquabacterium 3.05%</u> , <u>Gp4 (2.99%)</u> , Ohtaekwangia, <u>Haliscomenobacter (1.73%)</u> , <u>Luteimonas (1.65%)</u> , <u>Paracoccus (1.27%)</u> , <u>Altererythrobacter (1.18%)</u> , <u>Brevundimonas (1%)</u> | <u>Meganema (26%)</u> Ohtaekwangia, <u>Leadbetterella (6.16%)</u> , Planctomyces, <u>Pseudofulvimonas (2.78%)</u> , Schlesneria, <u>Gp4 (1.82%)</u> , Saccharibacteria_genera_inc_sed, Spartobacteria_genera_inc_sed, <u>Paracoccus (1.18%)</u> , Armatimonadetes_gp5 |
| 52 Major (>10%) Minor (>1%) | <u>Meganema (11.4%)</u> <u>Zoogloea (6.54%)</u> , Parcubacteria_genera_inc_sed, <u>Leadbetterella (3.62%)</u> , <u>Luteimonas (3.58%)</u> , Nannocystis, Pedobacter, <u>Thauera (1.86%)</u> , Ohtaekwangia, Blastocatella, Ilumatobacter, Flavobacterium, Proteiniphilum, <u>Hydrogenophaga (1.04%)</u> | <u>Meganema (17.7%)</u> <u>Amaricoccus (5.32%)</u> , <u>Luteimonas (2.49%)</u> , <u>Thauera (2.04%)</u> , Saccharibacteria_genera_inc_sed, Nannocystis, <u>Thermomonas (1.09%)</u> , <u>Paracoccus (1.33%)</u> , <u>Mycobacterium (1.05%)</u> , <u>Xanthobacter (1.03%)</u> , <u>Filomicrobium (1%)</u> | <u>Meganema (32.8%)</u> <u>Paracoccus (3.95%)</u> , <u>Amaricoccus (3.61%)</u> , <u>Leadbetterella (2.51%)</u> , Ohtaekwangia, <u>Hylemonella (1.97%)</u> , Ilumatobacter, <u>Luteimonas (1.56%)</u> , Mesorhizobium, <u>Hyphomicrobium (1.33%)</u> , <u>Pseudofulvimonas (1.06%)</u> , <u>Gp4 (1.11%)</u> | <u>Meganema (15.8%)</u> <u>Amaricoccus (4.2%)</u> , <u>Paracoccus (3.75%)</u> , Ohtaekwangia, <u>Luteimonas (2.24%)</u> , <u>Gp4 (2.11%)</u> , <u>Gp6 (1.54%)</u> , <u>Leadbetterella (1.48%)</u> , <u>Parvivaculum (1.23%)</u> , <u>Hyphomicrobium (1.15%)</u> , <u>Novosphingobium (1.15%)</u> , Nannocystis |
| 271 Major (>10%) Minor (>1%) | — <u>Zoogloea (9.9%)</u> , <u>Thauera (7.87%)</u> , <u>Meganema (4.95%)</u> , Proteiniphilum, Bacteroides, Sphaerochaeta | — <u>Thauera (9.61%)</u> , <u>Meganema (6.93%)</u> , <u>Zoogloea (5.45%)</u> , Proteiniphilum, <u>Dokdonella (1.55%)</u> , Bacteroides | <u>Zoogloea (24.3%)</u> <u>Meganema (6.92%)</u> , Bacteroides, Sphaerochaeta, Proteiniphilum, <u>Thauera (1.16%)</u> , <u>Haliscomenobacter (1.12%)</u> | — <u>Meganema (5.68%)</u> , <u>Gp4 (4.81%)</u> , <u>Haliscomenobacter (3.58%)</u> , Proteiniphilum, Parcubacteria_genera_inc_sed, <u>Amaricoccus (2.68%)</u> , <u>Thauera (2.31%)</u> , Oscillibacter, Hallella, Prostheco bacter, <u>Leadbetterella (1.31%)</u> , <u>Sphingomonas (1.13%)</u> |

potential as PHA producers in the respective Enrichment reactors are highlighted in Table 5 (bold and underlined). As shown, 21.5–49.9% of the MMC for genera present at >1% have the potential to synthesize PHA. Specifically pertaining to the most dominant genera observed (*Meganema*), its capabilities may be evaluated by considering the only species currently in the RDP database, namely *M. perideroedes*, as a proxy. *M. perideroedes* is a filamentous organism that was identified in activated sludge (Thomsen et al., 2006) and was shown to exhibit rapid substrate uptake (including acetate, propionate, and butyrate) using various electron acceptors (oxygen, nitrite, and nitrate) in addition to a high PHA-accumulation capacity (Kragelund et al., 2005; Thomsen et al., 2006). These metabolic characteristics of *M. perideroedes*, coupled with the observation of more than half of the major phylotypes identified having at least one member known to possess a subset of VFA assimilation or PHA synthesis, aligned with the observed bulk solution changes in the Enrichment reactors; the denitrification potential also aligned well with Enrichment reactor performance. *Thauera*, another prominent PHA-producing microbe that was observed in nearly all MMC at >1%, is also capable of denitrification (Morgan-Sagastume et al., 2008). The presence of denitrifying PHA-producing microorganisms fits well with the observed nitrogen

cycling, particularly in Enrichment reactors AE-4, -8, and -12. As a final note, the MMC contained filamentous bacteria (e.g., *Meganema*, *Haliscomenobacter*); with no settling phase incorporated into the SBR operation, such an outcome is not surprising.

Finally, considering MMC diversity as related to PHA production potential, some of the highest maximum PHA contents achieved (75–80% PHA (VSS basis) for waste feedstocks (Albuquerque et al., 2010; Carvalho et al., 2014) and upwards of 90% PHB (TSS basis) for synthetic substrates (Jiang et al., 2011; Johnson et al., 2009)) were achieved with MMC enrichments with low microbial diversity. Results from Hanson et al. (2016) for PHA production on sterilized dairy manure fermenter liquor further indicate a similar relationship. Thus, it could be suggested that lower microbial diversity in enriched MMCs may be favorable for fed-batch PHA production, particularly when increased microbial diversity is associated with more non-PHA producing bacteria – an observation other investigations have also made (Jiang et al., 2012; Queirós et al., 2014; Tamis et al., 2014). However, a similar analysis on this study's data was not so conclusive; no relationship was observed between MMC diversity and %PHA or PHA yield (data not shown). Applying a Bray-Curtis similarity analysis to the respective MMC, no discernable clustering by reactor was observed (Fig. S7 and Table S7). The

respective MMC did generally cluster by operational day, but significant dissimilarity existed. MMC in AE-4 and -8 exhibited the most similarity (80% on operational day 271; 76% on operational day 29), although similarity across reactors generally was less than 60%. Collectively, the microbial ecology results suggest functional redundancy across diverse MMC is realized in ADF-operated reactors fed a complex (waste-based) substrate.

4. Conclusions

Investigations were undertaken to evaluate the effect of aeration (controlled using the oxygen mass transfer coefficient, k_La) on feast-famine PHA synthesis by mixed microbial consortia fed VFA-rich fermented dairy manure; applied k_La values were 4, 8, 12, and 20 h^{-1} , and residual dissolved oxygen was measured as a response parameter. Assessment of PHA Enrichment reactors revealed no statistical effect from reduced aeration on rates of carbon uptake and storage. Indeed, regardless of the aeration state, all MMC exhibited a feast-famine response based on observed carbon cycling. While a typical feast-famine dissolved oxygen (DO) pattern was observed at maximum aeration, less resolution was observed at decreasing aeration rates, suggesting that DO may not be an optimal process monitoring parameter. Moreover, lower aeration states did appear to impair excess accumulation of PHA by MMC in the Production reactors. At lower aeration states, nitrogen cycling revealed that alternative electron acceptors (NO_2 , NO_3) sustained feast-famine PHA synthesis mechanisms; molecular investigations targeting AOBs and NOBs supported these observations. Next-generation sequencing analysis of the MMC revealed very diverse populations across the applied aeration states. Numerous and diverse genera observed in the respective Enrichment reactor MMCs are putative PHA producers, suggesting functional redundancy. Ultimately, results demonstrate that aeration can be controlled in waste-based ADF systems to sustain PHA production potential, while enriching for a diverse MMC that exhibits potential functional redundancy. Reduced aeration could enhance cost competitiveness of waste-based PHA production, with potential further benefits associated with nitrogen treatment.

Acknowledgements

The material presented and discussed herein is based upon work supported by i) the U.S. Department of Agriculture under Grant Number NIFA#2012-68002-19952, ii) the National Science Foundation under Grant Number CBET-1235885, iii) the Idaho Dairy-men's Association, and iv) an Institutional Development Award (IDeA) from the National Institute of General Medical Sciences of the National Institutes of Health under Grant Number P20GM103408. Any opinions, findings, and conclusions or recommendations expressed in this material are those of the authors and do not necessarily reflect the views of the funding agencies.

The authors greatly appreciate the efforts of Nicholas M. Guho, who prepared and executed workflows to evaluate the MiSeq results and generate the associated tables and figures.

Appendix A. Supplementary data

Supplementary data related to this article can be found at <http://dx.doi.org/10.1016/j.watres.2016.09.039>.

References

- Akiyama, M., Tsuge, T., Doi, Y., 2003. Environmental life cycle comparison of polyhydroxyalkanoates produced from renewable carbon resources by bacterial fermentation. *Polym. Degrad. Stabil.* 80 (1), 183–194.
- Albuquerque, M.G.E., Torres, C.A.V., Reis, M.A.M., 2010. Polyhydroxyalkanoate (PHA) production by a mixed microbial culture using sugar molasses: effect of the influent substrate concentration on culture selection. *Water Res.* 44 (11), 3419–3433.
- Albuquerque, M.G.E., Carvalho, G., Kragelund, C., Silva, A.F., Crespo, M.T.B., Reis, M.A.M., Nielsen, P.H., 2013. Link between microbial composition and carbon substrate-uptake preferences in a PHA-storing community. *ISME J.* 7 (1), 1–12.
- Anterrieu, S., Quadri, L., Geurkink, B., Dinkla, I., Bengtsson, S., Arcos-Hernandez, M., Alexandersson, T., Morgan-Sagastume, F., Karlsson, A., Hjort, M., Karabegovic, L., Magnusson, P., Johansson, P., Christensson, M., Werker, A., 2014. Integration of biopolymer production with process water treatment at a sugar factory. *New Biotechnol.* 31 (4), 308–323.
- APHA, AWWA, WEF, 2012. Standard Methods for the Examination of Water and Wastewater. AWWA.
- Bengtsson, S., Pisco, A.R., Johansson, P., Lemos, P.C., Reis, M.A.M., 2010a. Molecular weight and thermal properties of polyhydroxyalkanoates produced from fermented sugar molasses by open mixed cultures. *J. Biotechnol.* 147 (3–4), 172–179.
- Bengtsson, S., Pisco, A.R., Reis, M.A.M., Lemos, P.C., 2010b. Production of polyhydroxyalkanoates from fermented sugar cane molasses by a mixed culture enriched in glycogen accumulating organisms. *J. Biotechnol.* 145 (3), 253–263.
- Beun, J.J., Dircks, K., Van Loosdrecht, M.C.M., Heijnen, J.J., 2002. Poly- β -hydroxybutyrate metabolism in dynamically fed mixed microbial cultures. *Water Res.* 36 (5), 1167–1180.
- Braunegg, G., Sonnleitner, B., Lafferty, R.M., 1978. A rapid gas chromatographic method for the determination of poly- β -hydroxybutyric acid in microbial biomass. *Eur. J. Appl. Microbiol.* 6, 29–37.
- Braunegg, G., Lefebvre, G., Genser, K.F., 1998. Polyhydroxyalkanoates, biopolyesters from renewable resources: physiological and engineering aspects. *J. Biotechnol.* 65 (2–3), 127–161.
- Carvalho, G., Oehmen, A., Albuquerque, M.G.E., Reis, M.A.M., 2014. The relationship between mixed microbial culture composition and PHA production performance from fermented molasses. *New Biotechnol.* 31 (4), 257–263.
- Chen, G.-Q., Patel, M.K., 2012. Plastics derived from biological sources: present and future: a technical and environmental review. *Chem. Rev.* 112 (4), 2082–2099.
- Clesceri, L.S., Greenberg, A.E., Eaton, A.D., 1998. Standard Methods for Examination of Water and Wastewater. American Public Health Association, Washington D.C.
- Coats, E.R., Searcy, E., Feris, K., Shrestha, D., McDonald, A.G., Briones, A., Magnusson, T., Prior, M., 2013. An integrated 2-stage anaerobic digestion and biofuel production process to reduce life cycle GHG emissions from U.S. dairies. *BioFPR* 7 (4), 459–473.
- Dias, J.M.L., Serafim, L.S., Lemos, P.C., Reis, M.A.M., Oliveira, R., 2005. Mathematical modelling of a mixed culture cultivation process for the production of polyhydroxybutyrate. *Biotechnol. Bioeng.* 92 (2), 209–222.
- Dias, J.M.L., Lemos, P.C., Serafim, L.S., Oliveira, C., Eiroa, M., Albuquerque, M.G.E., Ramos, A.M., Oliveira, R., Reis, M.A., 2006. Recent advances in polyhydroxyalkanoate production by mixed aerobic cultures: from the substrate to the final product. *Macromol. Biosci.* 6, 885–906.
- Dionisi, D., Majone, M., Tandoi, V., Beccari, M., 2001. Sequencing batch reactor: influent of periodic operation on performance of activated sludges in biological wastewater treatment. *Ind. Eng. Chem. Res.* 40, 5110–5119.
- Dionisi, D., Renzi, V., Majone, M., Beccari, M., Ramadori, R., 2004. Storage of substrate mixtures by activated sludges under dynamic conditions in anoxic or aerobic environments. *Water Res.* 38 (8), 2196–2206.
- Dionisi, D., Majone, M., Vallini, G., Di Gregorio, S., Beccari, M., 2006. Effect of the applied organic load rate on biodegradable polymer production by mixed microbial cultures in a sequencing batch reactor. *Biotechnol. Bioeng.* 93 (1), 76–88.
- Dionisi, D., Majone, M., Vallini, G., DiGregorio, S., Beccari, M., 2007. Effect of the length of the cycle on biodegradable polymer production and microbial community selection in a sequencing batch reactor. *Biotechnol. Prog.* 23 (5), 1064–1073.
- Fernández-Dacosta, C., Posada, J.A., Kleerebezem, R., Cuellar, M.C., Ramirez, A., 2015. Microbial community-based polyhydroxyalkanoates (PHAs) production from wastewater: techno-economic analysis and ex-ante environmental assessment. *Bioresour. Technol.* 185, 368–377.
- García-Ochoa, F., Gómez, E., 2009. Bioreactor scale-up and oxygen transfer rate in microbial processes: an overview. *Biotechnol. Adv.* 27 (2), 153–176.
- Gurieff, N., Lant, P., 2007. Comparative life cycle assessment and financial analysis of mixed culture polyhydroxyalkanoate production. *Bioresour. Technol.* 98 (17), 3393–3403.
- Hanson, A.J., Guho, N.M., Paszczynski, A.J., Coats, E.R., 2016. Community proteomics provides functional insight into polyhydroxyalkanoate production by a mixed microbial culture cultivated on fermented dairy manure. *Appl. Biochem. Biotechnol.* 1–20.
- Hill, T.C.J., Walsh, K.A., Harris, J.A., Moffett, B.F., 2003. Using ecological diversity measures with bacterial communities. *FEMS Microbiol. Ecol.* 43 (1), 1–11.
- Jiang, Y., Marang, L., Kleerebezem, R., Muyzer, G., van Loosdrecht, M.C.M., 2011. Polyhydroxybutyrate production from lactate using a mixed microbial culture. *Biotechnol. Bioeng.* 108 (9), 2022–2035.
- Jiang, Y., Marang, L., Tamis, J., van Loosdrecht, M.C.M., Dijkman, H., Kleerebezem, R., 2012. Waste to resource: converting paper mill wastewater to bioplastic. *Water Res.* 46 (17), 5517–5530.
- Johnson, K., Jiang, Y., Kleerebezem, R., Muyzer, G., van Loosdrecht, M.C.M., 2009.

- Enrichment of a mixed bacterial culture with a high polyhydroxyalkanoate storage capacity. *Biomacromolecules* 10 (4), 670–676.
- Kragelund, C., Nielsen, J.L., Thomsen, T.R., Nielsen, P.H., 2005. Ecophysiology of the filamentous alphaproteobacterium *Meganema perideroedes* in activated sludge. *FEMS Microbiol. Ecol.* 54 (1), 111–122.
- Leininger, S., Urich, T., Schlöter, M., Schwark, L., Qi, J., Nicol, G.W., Prosser, J.I., Schuster, S.C., Schleper, C., 2006. Archaea predominate among ammonia-oxidizing prokaryotes in soils. *Nature* 442 (7104), 806–809.
- Lemoigne, M., 1926. Produits de deshydratation et de polymérisation de l'acide α -oxobutyrique. *Bull. Soc. Chem. Biol. Paris* 8, 770–782.
- Lemos, P.C., Levantesi, C., Serafim, L.S., Rossetti, S., Reis, M.A.M., Tandoi, V., 2008. Microbial characterisation of polyhydroxyalkanoates storing populations selected under different operating conditions using a cell-sorting RT-PCR approach. *Appl. Microbiol. Biotechnol.* 78 (2), 351–360.
- Luzier, W.D., 1992. Materials derived from biomass/biodegradable materials. *PNAS* 89, 839–842.
- Madison, L.L., Huisman, G.W., 1999. Metabolic engineering of poly (3-hydroxyalkanoates): from DNA to plastic. *Microbiol. Mol. Biol. Rev.* 63 (1), 21–53.
- Maehara, A., Taguchi, S., Nishiyama, T., Yamane, T., Doi, Y., 2002. A repressor protein, PhaR, regulates polyhydroxyalkanoate (PHA) synthesis via its direct interaction with PHA. *J. Bacteriol.* 184 (14), 3992–4002.
- Magoc, T., Salzberg, S.L., 2011. FLASH: fast length adjustment of short reads to improve genome assemblies. *Bioinformatics* 27 (21), 2957–2963.
- Majone, M., Massanisso, P., Carucci, A., Lindrea, K., Tandoi, V., 1996. Influence of storage on kinetic selection to control aerobic filamentous bulking. *Water Sci. Technol.* 34 (5–6), 223–232.
- Majone, M., Beccari, M., Di Gregorio, S., Dionisi, D., Vallini, G., 2006. Enrichment of activated sludge in a sequencing batch reactor for polyhydroxyalkanoate production. *Water Sci. Technol.* 54 (1), 119–128.
- Marang, L., Jiang, Y., van Loosdrecht, M.C.M., Kleerebezem, R., 2013. Butyrate as preferred substrate for polyhydroxybutyrate production. *Bioresour. Technol.* 142, 232–239.
- McIlroy, S.J., Saunders, A.M., Albertsen, M., Nierychlo, M., McIlroy, B., Hansen, A.A., Karst, S.M., Nielsen, J.L., Nielsen, P.H., 2015. MIDAS: the Field Guide to the Microbes of Activated Sludge. Database 2015.
- Moralejo-Gárate, H., Kleerebezem, R., Mosquera-Corral, A., van Loosdrecht, M.C.M., 2013. Impact of oxygen limitation on glycerol-based biopolymer production by bacterial enrichments. *Water Res.* 47 (3), 1209–1217.
- Morgan-Sagastume, F., Nielsen, J.L., Nielsen, P.H., 2008. Substrate-dependent denitrification of abundant probe-defined denitrifying bacteria in activated sludge. *FEMS Microbiol. Ecol.* 66 (2), 447–461.
- Muyzer, G., de Waal, E.C., Uitterlinden, A.G., 1993. Profiling of complex microbial populations by denaturing gradient gel electrophoresis analysis of polymerase chain reaction-amplified genes coding for 16S rRNA. *Appl. Environ. Microbiol.* 59 (3), 695–700.
- Padermshoke, A., Katsumoto, Y., Sato, H., Ekgasitb, S., Nodad, I., Ozakia, Y., 2004. Surface melting and crystallization behavior of polyhydroxyalkanoates studied by attenuated total reflection infrared spectroscopy. *Polymer* 45, 6547–6554.
- Passero, M.L., Cragin, B., Hall, A.R., Staley, N., Coats, E.R., McDonald, A.G., Feris, K., 2014. Ultraviolet radiation pre-treatment modifies dairy wastewater, improving its utility as a medium for algal cultivation. *Algal Res.* 6 (Part A(0)), 98–110.
- Queirós, D., Rossetti, S., Serafim, L.S., 2014. PHA production by mixed cultures: a way to valorize wastes from pulp industry. *Bioresour. Technol.* 157, 197–205.
- Ramakers, C., Ruijter, J.M., Deprez, R.H.L., Moorman, A.F.M., 2003. Assumption-free analysis of quantitative real-time polymerase chain reaction (PCR) data. *Neurosci. Lett.* 339 (1), 62–66.
- Reis, M.A.M., Serafim, L.S., Lemos, P.C., Ramos, A.M., Aguiar, F.R., van Loosdrecht, M.C.M., 2003. Production of polyhydroxyalkanoates by mixed microbial cultures. *Bioprocess Biosyst. Eng.* 25, 377–385.
- Rotthauwe, J.H., Witzel, K.P., Liesack, W., 1997. The ammonia monooxygenase structural gene *amoA* as a functional marker: molecular fine-scale analysis of natural ammonia-oxidizing populations. *Appl. Environ. Microbiol.* 63 (12), 4704–4712.
- Rudnik, E., 2008. *Compostable Polymer Materials*. Elsevier, Oxford, UK.
- Serafim, L.S., Lemos, P.C., Oliveira, R., Reis, M.A.M., 2004. Optimization of polyhydroxybutyrate production by mixed microbial cultures submitted to aerobic dynamic feeding conditions. *Biotechnol. Bioeng.* 87 (2), 145–160.
- Serafim, L.S., Lemos, P.C., Albuquerque, M.G.E., Reis, M.A.M., 2008. Strategies for PHA production by mixed cultures and renewable waste materials. *Appl. Microbiol. Biotechnol.* 81, 615–628.
- Shen, J., Song, N., Williams, C.J., Brown, C.J., Yan, Z., Xu, C., Forney, L.J., 2016. Effects of low dose estrogen therapy on the vaginal microbiomes of women with atrophic vaginitis. *Sci. Rep.* 6, 24380.
- Shen, L., Worrell, E., Patel, M., 2010. Present and future development in plastics from biomass. *BioFPR* 4, 25–40.
- Stowe, E.J., Coats, E.R., Brinkman, C.K., 2015. Dairy manure resource recovery utilizing two-stage anaerobic digestion - implications of solids fractionation. *Bioresour. Technol.* 198, 237–245.
- Tamis, J., Lukov, K., Jiang, Y., van Loosdrecht, M.C., Kleerebezem, R., 2014. Enrichment of *Plasticumulans acidivorans* at pilot-scale for PHA production on industrial wastewater. *J. Biotechnol.* 192, 161–169.
- Tchobanoglous, G., Stensel, H.D., Tsuchihashi, R., Burton, F., 2014. *Wastewater Engineering: Treatment and Resource Recovery*. Metcalf & Eddy/AECOM, New York, NY.
- Third, K.A., Burnett, N., Cord-Ruwisch, R., 2003a. Simultaneous nitrification and denitrification using stored substrate (PHB) as the electron donor in an SBR. *Biotechnol. Bioeng.* 83 (6), 706–720.
- Third, K.A., Newland, M., Cord-Ruwisch, R., 2003b. The effect of dissolved oxygen on PHB accumulation in activated sludge cultures. *Biotechnol. Bioeng.* 82 (2), 238–250.
- Third, K.A., Sepmaniam, S., Tonkovic, Z., Newland, M., Cord-Ruwisch, R., 2004. Optimisation of storage driven denitrification by using on-line specific oxygen uptake rate monitoring during SND in a SBR. *Water Sci. Technol.* 50 (10), 171–180.
- Thomsen, T.R., Blackall, L.L., de Muro, M.A., Nielsen, J.L., Nielsen, P.H., 2006. *Meganema perideroedes* gen. nov., sp. nov., a filamentous alphaproteobacterium from activated sludge. *Int. J. Syst. Evol. Microbiol.* 56, 1865–1868.
- Valentino, F., Karabegovic, L., Majone, M., Morgan-Sagastume, F., Werker, A., 2015. Polyhydroxyalkanoate (PHA) storage within a mixed-culture biomass with simultaneous growth as a function of accumulation substrate nitrogen and phosphorus levels. *Water Res.* 77, 49–63.
- van Loosdrecht, M.C.M., Pot, M.A., Heijnen, J.J., 1997. Importance of bacterial storage polymers in bioprocesses. *Water Sci. Technol.* 35 (1), 41–47.
- Van Wegen, R.J., Ling, Y., Middelberg, A.P.J., 1998. Industrial production of PHAs using *Escherichia coli*: an economic analysis. *Trans. IChemE* 76 (3), 417–426.
- Villano, M., Beccari, M., Dionisi, D., Lampis, S., Miccheli, A., Vallini, G., Majone, M., 2010. Effect of pH on the production of bacterial polyhydroxyalkanoates by mixed cultures enriched under periodic feeding. *Proc. Biochem.* 45 (5), 714–723.
- Waller, J.L., Green, P.G., Loge, F.J., 2012. Mixed-culture polyhydroxyalkanoate production from olive oil mill pomace. *Bioresour. Technol.* 120, 285–289.
- Wang, Q., Garrity, G.M., Tiedje, J.M., Cole, J.R., 2007. Naïve bayesian classifier for rapid assignment of rRNA sequences into the new bacterial taxonomy. *Appl. Environ. Microbiol.* 73 (16), 5261–5267.
- Winkler, M., Coats, E.R., Brinkman, C.K., 2011. Advancing post-anoxic denitrification for biological nutrient removal. *Water Res.* 45 (18), 6119–6130.
- Yates, M.R., Barlow, C.Y., 2013. Life cycle assessments of biodegradable, commercial biopolymers-A critical review. *Resour. Conserv. Recycl.* 78, 54–66.